Quantifying sediment sources in a lowland agricultural catchment pond using ^{137}Cs activities and radiogenic ^{87}Sr/ ^{86}Sr ratios

Marion Le Gall, O. Evrard, Anthony Foucher, J. Patrick Laceby, Sébastien Salvador-Blanes, François Thil, Arnaud Dapoigny, Irène Lefèvre, Olivier Cerdan, Sophie Ayrault

Quantifying sediment sources in a lowland agricultural catchment pond using ^{137}Cs activities and radiogenic ^{87}Sr/^{86}Sr ratios

Marion Le Gall[a*], Olivier Evrard[a], Anthony Foucher[b], J. Patrick Laceby[a], Sébastien Salvador-Blanes[b], François Thil[a], Arnaud Dapoigny[a], Irène Lefèvre[a], Olivier Cerdan[c], Sophie Ayrault[a]

[a] *Laboratoire des Sciences et de l'Environnement, UMR 8212 (CEA/CNRS/UVSQ), Université Paris-Saclay, Domaine du CNRS, Avenue de la Terrasse, 91198 Gif-sur-Yvette Cedex, France*

[b] *E.A 6293, Laboratoire GéoHydrosystèmes Continentaux (GéHCO), Université F. Rabelais de Tours, Faculté des Sciences et Techniques, Parc de Grandmont, 37200 Tours, France*

[c] *Département Risques et Prévention, Bureau de Recherches Géologiques et Minières, 3 avenue Claude Guillemin, 45060 Orléans, France*

Highlights

- Surface sources supplied the majority of pond and core sediment.
- Lithological sources were well mixed in surface pond sediment.
- Lithological sources varied through time in the sediment core.
- Temporal lithological fluctuations likely resulted from landscape modifications.
- Understanding sediment dynamics is important in agricultural drained catchments.

Abstract

Soil erosion often supplies high sediment loads to rivers, degrading water quality and contributing to the siltation of reservoirs and lowland river channels. These impacts are exacerbated in agricultural catchments where modifications in land management and agricultural practices were shown to accelerate sediment supply. In this study, sediment sources were identified with a novel tracing approach combining cesium (^{137}Cs) and strontium isotopes (^{87}Sr/^{86}Sr) in the Louroux pond, at the outlet of a lowland cultivated catchment (24 km², Loire River basin, France) representative of drained agricultural areas of Northwestern Europe.

Surface soil (n=36) and subsurface channel bank (n=17) samples were collected to characterize potential sources. Deposited sediment (n=41) was sampled across the entire surface of the pond to examine spatial variation in sediment deposits. In addition, a 1.10 m sediment core was sampled in the middle of the pond to reconstruct source variations throughout time. ^{137}Cs was used to discriminate between surface and subsurface sources, whereas ^{87}Sr/^{86}Sr ratios discriminated between lithological sources. A distribution modeling approach quantified the relative contribution of these sources to the sampled sediment.

Results indicate that surface sources contributed to the majority of pond (μ 82%, σ 1%) and core (μ 88%, σ 2%) sediment with elevated subsurface contributions modeled near specific sites close to the banks of the Louroux pond. Contributions of the lithological sources were well mixed in surface sediment across the pond (i.e., carbonate sediment contribution, μ 48%, σ 1% and non-carbonate sediment contribution, μ 52%, σ 3%) although there were significant variations of these source contributions modeled for the sediment core between 1955 and 2013. These fluctuations reflect both the progressive implementation of land consolidation schemes in the catchment and the eutrophication of the pond.

This original sediment fingerprinting study demonstrates the potential of combining radionuclide and strontium isotopic geochemistry measurements to quantify sediment sources in cultivated catchments.

Keywords: fallout radionuclides, radiocesium, strontium isotopes, sediment tracing, fingerprinting

1 Introduction

Soil erosion is a major environmental threat worldwide. This process of detachment, transportation and deposition of soil particles by rainfall and runoff particularly affects agricultural areas of Northwestern Europe (Boardman, 1993; Evrard et al., 2007; Le Bissonnais et al., 2005). Soil erosion not only results in decreasing soil fertility and crop yields (Bakker et al., 2004; Boardman et al., 2003), it often supplies high sediment loads to river networks (Owens et al., 2005).

High suspended sediment loads may increase turbidity and result in the sedimentation of downstream reservoirs and lowland river channels (Devlin et al., 2008; Vörösmarty et al., 2003). Sediment may also transport nutrients and contaminants including phosphorous, pesticides, persistent organic pollutants, heavy metals, pathogens and radionuclides (Ayrault et al., 2012; Chartin et al., 2013; Gateuille et al., 2014; Horowitz, 2008). Therefore, understanding spatial and temporal variations of sediment sources is useful for managing the supply of sediment and contaminants in river systems.

Agricultural landscapes have been extensively modified by human activities during the last century to facilitate mechanization and increase crop yields (Dotterweich, 2013; García-Ruiz, 2010; Valentin et al., 2005). In wetlands, tile drain outlets have been installed and channels have been created to evacuate excess water. Although these alterations resulted in substantial increases in soil erosion and downstream sediment loads, there has been limited research quantifying erosion and sediment transport in these areas (Foucher et al., 2014; Russell et al., 2001; Sogon et al., 1999; Walling et al., 2002). Furthermore, even fewer studies (e.g. Russell et al., 2001) have examined the relative contribution of different sediment sources in these drained lowland agricultural catchments.

Quantifying sediment sources is important to target efficient management measures that reduce sediment supply in catchments. Sediment fingerprinting techniques are therefore increasingly applied to determine sediment sources and pathways in catchments and thus inform management interventions (Collins and Walling, 2002; Koiter et al., 2013; Walling, 2005). Sediment fingerprinting techniques often trace radionuclide, geochemical, and mineralogical soil and sediment properties (Collins et al., 2012; Evrard et al., 2016; Evrard et al., 2011; Olley et al., 1993; Walling et al., 2008). Sediment color or infrared spectroscopy (Martínez-Carreras et al., 2010; Poulenard et al., 2012), plant pollen (Brown et al., 2008), soil enzymes (Nosrati et al., 2011), sediment magnetic properties (Hatfield and Maher, 2009; Hatfield et al., 2008) or methyl esters (Banowetz et al., 2006) have also been used to discriminate between potential sediment sources. For a review of the strengths and limitations of different tracer properties and tracing approaches, please see Collins and Walling (2004), Davis and Fox (2009), Guzmán et al. (2013), Haddadchi et al., (2013), and Koiter et al. (2013).

The choice of discriminant properties is often guided by the sources supplying sediment. For example, fallout radionuclides discriminate between surface and subsurface sources (Owens and Walling, 2002; Smith and Dragovich, 2008). ^{137}Cs ($t_{1/2}$=30 years) is an artificial radionuclide, produced by thermonuclear tests in the 1950s and 1960s, the Chernobyl accident that affected Northwestern Europe in 1986 and the Fukushima Dai-ichi Nuclear Power Plant accident in 2011. Radiocesium is strongly bound to fine particles (He and Walling, 1996). In undisturbed soil profiles, ^{137}Cs concentrations are the highest at the surface before decreasing exponentially with depth (Mabit et al., 2008; Olley et al., 2013). Accordingly, sediment originating from the soil surface or the ploughed layer will contain higher ^{137}Cs concentrations compared to sediment originating from subsurface sources (e.g. channel bank and gully erosion) which will be depleted in ^{137}Cs. Therefore, it is possible

to quantify the relative contribution of surface and subsurface sources by modeling ^{137}Cs soil and sediment concentrations (Caitcheon et al., 2012; Olley et al., 2013).

In comparison, strontium isotopes ($^{87}Sr/^{86}Sr$) were shown to be effective tracers of water, soil, sediment and biological material in the environment as they are not fractionated by chemical or biological processes (Aberg, 1995; Graustein, 1989). The abundance of ^{87}Sr produced by the radioactive decay of ^{87}Rb (expressed as the $^{87}Sr/^{86}Sr$ ratio) varies with rock type and its formation age (Négrel and Roy, 1998; Yasuda et al., 2014). Accordingly, strontium isotopic ratios reflect catchment lithology and thus they have been used to trace the geological sources of soils, suspended particulate matter and riverine water in catchments (Faure, 1986).

Strontium isotopic ratios have mainly been measured in the dissolved load (Gaillardet et al., 1997; Grosbois et al., 2000; Pande et al., 1994) to identify and quantify chemical weathering fluxes in major rivers (e.g. the Amazon, Congo, Garonne, Indus, Loire, Rhine Rivers catchments) and to provide information about surface and subsurface water circulations (Bakari et al., 2013; Brenot et al., 2008; Eikenberg et al., 2001; Petelet-Giraud et al., 2007), water-rock interactions (Aubert et al., 2001; Blum et al., 1994) or seawater dynamics (Jørgensen et al., 2008). Strontium isotopic ratios were also measured in suspended matter to identify the sources of particles transported in the ocean (Asahara et al., 1999; Goldstein and Jacobsen, 1988), in estuarine (Douglas et al., 2003; Smith et al., 2009) and fluvial systems (Asahara et al., 2006; Douglas et al., 1995; Négrel and Grosbois, 1999; Viers et al., 2000; Wasson et al., 2002). Despite their use in investigations of particulate material dynamics at large catchment scales, few studies investigated spatial and temporal variations of sediment sources with strontium isotopic ratios in small agricultural catchments (<50 km²). Small catchment scale research is important for improving our understanding of the impact of land use and farming practice changes on sediment dynamics.

In this study, sediment sources are identified and quantified through the combination of ^{137}Cs and $^{87}Sr/^{86}Sr$ ratio measurements on soil and sediment collected in the Louroux catchment (24 km²- Loire River basin, France), representative of drained, lowland, cultivated areas of Northwestern Europe. The Louroux pond, at the catchment outlet, is significantly impacted by sedimentation from increased sediment yields. Intense modifications in agricultural practices and land use in the catchment resulted in the excessive transport of fine sediment that was predominantly deposited in the Louroux pond. Fine sediment also transfers particulate-bound nutrients and contaminants and degraded water quality. As water quality may be directly impacted by this excess supply of sediment in this catchment, research is required to better understand sediment source dynamics in order to meet the requirements of the EU Water Framework Directive.

In this agricultural catchment, sediment surface sources were defined as topsoil material eroded from the cropland whereas subsurface sources were defined as material eroded from channel banks. Surface sources were shown to dominate (99 ± 1%) the supply of suspended matter transiting this catchment's rivers during flood events in 2013 (Foucher et al., 2015). However, the dominance of surface source contributions to sediment deposited throughout the pond and over a longer temporal period requires further investigation. Furthermore, information on the main spatial sources of sediment in the Louroux pond is required. To investigate spatial and temporal variations in sediment sources, ^{137}Cs concentrations and $^{87}Sr/^{86}Sr$ ratios were measured to estimate the relative contributions of surface, subsurface and lithological sources to multiple short sediment cores (i.e. < 10 cm) sampled throughout the Louroux pond as well one long sediment core (i.e. 1.1 m) sampled in the central pond depression.

2 Material and methods

2.1 Study site

The Louroux catchment (24 km²) is a small agricultural lowland basin with elevation ranging between 99 and 127 m and a mean slope of 0.4 %. The climate is temperate oceanic with a mean annual rainfall of 696 mm (Tours, data from Météo France, 2015). Cropland is the main land use (78%) followed by grassland (18%) and woodland (4%) (Corine Land Cover 2006 data). According to a geological survey, the lithology consists of post-Helvetian sand and continental gravels (32%), Senonian flint clays (23%), Quaternary loess (18%), Helvetian shelly sands (18%), Ludian Touraine lacustrine limestones (6%) and Eocene silicic conglomerates (2%) (Fig. S1) (Rasplus et al., 1982). These lithologies were regrouped in two classes (Le Gall et al., under review): a southern carbonate area composed of Touraine Lacustrine limestone and shelly limestone, and a northern non-carbonate grouping of the remaining lithologies (Fig. 1a).

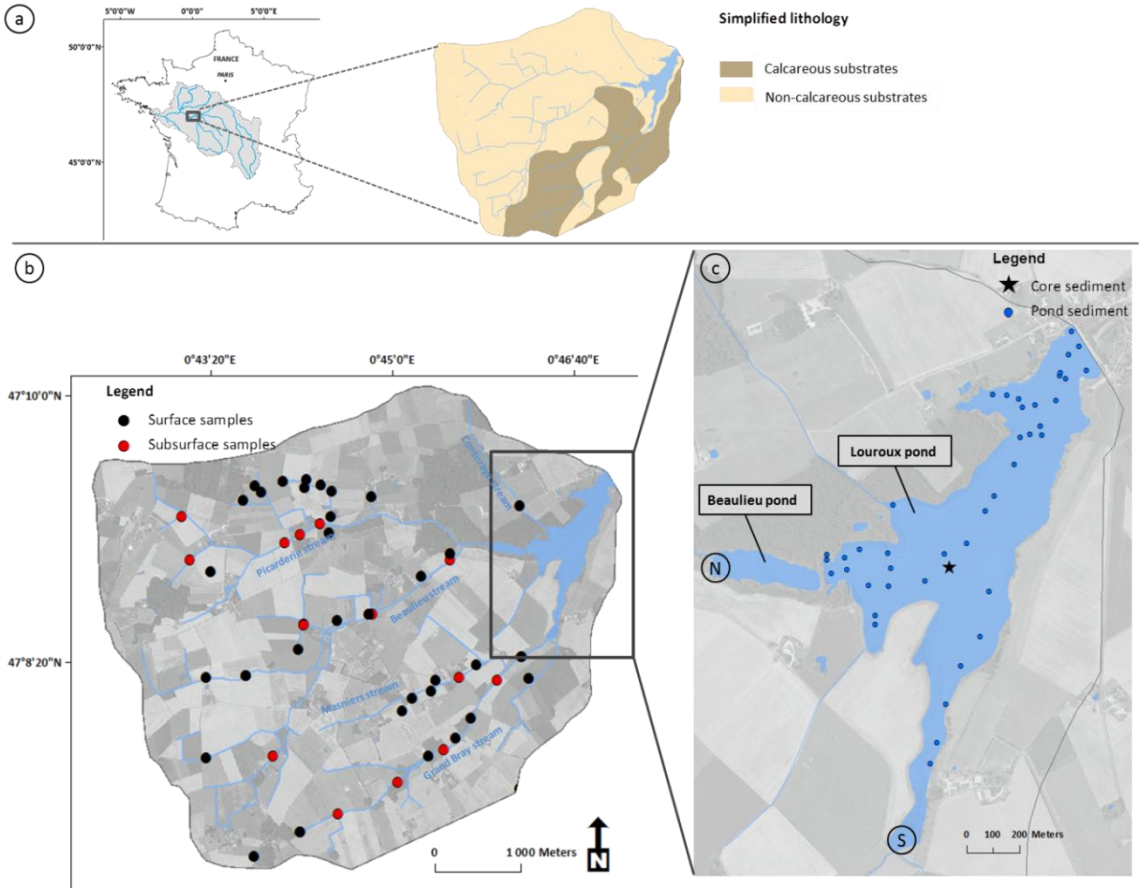

Fig. 1. Map of the Louroux catchment in the Loire River basin (France) along with the simplified lithological map of the area (Le Gall et al., under review) (a) and the locations of surface and subsurface source (b), pond and core sediment (c) samples location. N and S correspond to the northern and southern inlets of the main tributaries.

In the Louroux catchment, land consolidation started in the 1950s. Channels were created and others modified. More than 220 tile drain outlets were installed to drain soils and facilitate intensive crop farming. As a result, soil erosion and sediment fluxes strongly increased, contributing to the siltation of the river network, the Beaulieu pond (3 ha – nearly filled), and the Louroux pond (52 ha) (Fig. 1c). Foucher et al. (2014) showed that terrigeneous inputs to the Louroux pond reached maximum rates of 2100 t km^{-2} yr^{-1} between 1945 and 1960, before decreasing to lower rates (90-102 t km^{-2} yr^{-1}) since 2000.

2.2 Sampling

2.2.1 Soil and channel bank sampling

Soil and channel bank samples were collected between January 2013 and April 2014. Sampling concentrated on cropland, as soil erosion was shown to be negligible under grassland and forest in similar environments (Cerdan et al., 2010). Surface sources (n=36) were collected by scraping the top 2-3cm layer of soil and subsurface sources (n=17) by scraping a 2-3cm layer of the sidewall from eroding channel banks (Fig. 1b). Each of these surface and subsurface source samples was composed of five sub-samples. A plastic spatula was used to collect samples and avoid potential metal contamination.

2.2.2 Louroux Pond sediment sampling

Surface samples of deposited pond sediment (n=41) were collected in September 2012 using a floating platform and a short (top 0-10 cm) gravitational corer UWITEC (Ø 90mm) during a period of low water level (see graphical abstract). Attention was paid to collect the most recent deposits following a random location sampling technique. A longer sediment core was collected in the central depression of the pond (1.10 m length) in March 2013, at the confluence between the Grand Bray and Beaulieu streams (Fig. 1c). The sediment core was dated in a previous study using an age depth model based on fallout radionuclide measurements (^{137}Cs and $^{210}Pb_{xs}$) (Foucher et al., 2014). In the remainder of the text, dates attributed to the successive sediment core layers are used to facilitate the interpretation of the core results. Carbonate outcrops (n=3), shelly sand (n=1), and three types of fertilizers (N, 33.5/ P.K, 25-25/ N.P.K, 15-15-15) commonly used by farmers in this catchment were also sampled to characterize their strontium isotopic signatures.

2.3 Sample processing and laboratory analysis

2.3.1 Gamma spectrometry measurements

Soil (n=36), channel bank (n=17) and sediment (n=41) samples were dried at 40°C and sieved to 2 mm before analysis. For radionuclide measurements, approximately 80 g of material was analyzed. ^{137}Cs (662 keV) activities were determined by gamma spectrometry using low background N and P type GeHP detectors (Canberra and Ortec) at the Laboratoire des Sciences du Climat et de l'Environnement. Measured activities were decay-corrected to the sampling date and provided with 2σ-errors. Th concentrations (mg kg^{-1}) were calculated from ^{228}Th activity concentrations. Assuming that ^{232}Th and it daughter products were in secular equilibrium, ^{228}Th activities were calculated using the average between the gamma rays of two of its daughter products, ^{212}Pb (239 keV) and ^{208}Tl (583 keV). Counting efficiencies and reliability were conducted using certified International Atomic Energy Agency (IAEA) standards (IAEA-444, 135, 375, RGU-1 and RGTh-1) prepared in the same containers as the samples. Uncertainties on radionuclides activities were ca. 5% for ^{228}Th, and up to 10% for ^{137}Cs. Based on ^{228}Th activities, the total Th concentration (mg kg^{-1}) of sediment samples was calculated using the universal law of radioactive decay.

2.3.2 Thorium particle size correction for ^{137}Cs activities

As ^{137}Cs is strongly bound to fine particles, potential particle size differences between sources and sediment may prevent their direct comparison. To avoid errors in the estimation of source contributions, the impacts of particle size on sediment properties must be carefully addressed. As an

alternative to a specific surface area (SSA) derived correction, a thorium correction was effectively applied by Foucher et al. (2015) in the Louroux pond catchment. These authors demonstrated that thorium-corrected particle size corrections produced globally better results compared to SSA corrections in this catchment.

The Th correction factor was calculated based on the variations of Th and ^{137}Cs concentrations in each sediment sample and each source sample (Eq. 1) compared to their mean Th and ^{137}Cs concentrations of the considered source.

$$Th\ sediment\ correction\ factor = \frac{{[Th]_{i,j}}/{[Th]_{mean\ source(s)}}}{{[^{137}Cs]_{i,j}}/{[^{137}Cs]_{mean\ source(s)}}} \quad \text{(Eq. 1)}$$

where $[Th]_i$ and $[^{137}Cs]_i$ are the respective thorium and cesium concentration of each individual sediment sample (i), and $[Th]_{mean\ source(s)}$ and $[^{137}Cs]_{mean\ source(s)}$ are the respective thorium and cesium concentrations of both surface and subsurface samples when applied to each sediment sample while $[Th]_j$ and $[^{137}Cs]_j$ are the respective thorium and cesium concentrations of each individual source sample (j) (i.e. surface or subsurface samples) and $[Th]_{mean\ source(s)}$ and $[^{137}Cs]_{mean\ source(s)}$ are the respective thorium and cesium mean concentrations of each source when respectively applied to surface and subsurface samples. Corrected ^{137}Cs concentrations were calculated by dividing each measured ^{137}Cs concentration of each individual sample by the associated Th correcting factor.

2.3.3 Geochemical measurements

A selection of 31 surface sediment samples and 20 core sediment samples were analyzed for strontium isotopes. As recommended in several sediment fingerprinting studies (Collins and Walling, 2002; Motha et al., 2003; Tiecher et al., 2015; Walling et al., 2000), geochemical measurements were performed on the <63 µm fraction of material, obtained by dry-sieving. Sieving samples to the <63um fraction theoretically allows for a more direct comparison between sediment and potential sources elemental concentrations, as it is assumed that this size fraction corresponds to the bulk of the sediment.

Mineralization and selective extraction of the "exchangeable and carbonate" fraction

Details of the mineralization of source, sediment, carbonate rocks and fertilizer samples are given in Supplementary Material. Approximately 100 mg or 125 mg of material was dissolved by the successive addition of HF (47-51%), $HClO_4$ (65-71%), HCl (34-37%) and HNO_3 (67%) in closed Teflon vessels on hot plates. Proportions of reagents used and durations varied according to the sample nature.

Selective extractions using diluted acetic acid (F1 fraction of the BCR protocol) were performed to characterize the $^{87}Sr/^{86}Sr$ signature and composition of the exchangeable/carbonate fraction of sediment samples (Pueyo et al., 2001). Selective extractions of the exchangeable and carbonate phase (F1) were performed to evaluate the amount of calcium extracted and to characterize the $^{87}Sr/^{86}Sr$ signature of the exchangeable/carbonate fraction of sediment samples. This fraction corresponds to the metals affected by sorption and desorption effects (bound to particles) and/or (the elements) associated with carbonates. The selective extraction procedure was adapted from the BCR protocol (Rauret et al., 1999). 20 mL of a solution of acetic acid (0.11 mol L^{-1}) was added to approximately 500 mg of sediment in a centrifuge tube and was shaken for 16 h at room

temperature. The extractant solution was separated from the residue by centrifugation (4000 rpm min^{-1} during 20 minutes) and stored at 4°C before analysis. Reproducibility of the extraction was controlled through triplicate analyses of core sediment samples (n=8). These sediment samples were selected to cover the $^{87}Sr/^{86}Sr$ ratio variations observed in the <63 µm fraction of all core sediment samples. Results will be presented as the average strontium concentrations and $^{87}Sr/^{86}Sr$ ratios measured for each triplicate.

Elemental concentrations and strontium isotopic analyses

Major and trace element concentrations (Na, Mg, K, Ca, Rb, Sr, Zn) were analyzed in mineralized solutions using an inductively coupled plasma quadrupolar mass spectrometer (ICP-QMS) (X-Series, CCT II^+ Thermoelectron, France). Internal standards (Re, Rh and In; SPEX, SCP Science, France) were used to correct for instrumental drift and plasma fluctuation. To limit interference, analysis was performed using a collision cell technology (CCT) which introduces a supplementary gas mixture of H_2 (7%) and He (93%) for the determination of Zn, Rb, and Sr concentrations.

A certified river water sample (SRM 1640a, NIST, Gaithersburg, USA) was used to control the ICP-MS calibration. The overall quality of ICP-MS measurements was controlled by analyzing a certified lake sediment material (IAEA lake sediment SL1). These standards were checked routinely during analysis (every 15-25 samples). Good agreement was observed between the data obtained and the certified values (n=91 for SL-1 measurements). In the particulate compartment, analytical uncertainties did not exceed 10% (except for Ca, with a maximum analytical error of 13%).

Chemical separation of strontium from rubidium and calcium was performed using a cation-exchange procedure. More details are given in Supplementary Material. $^{87}Sr/^{86}Sr$ ratios were determined using a Thermo Finnigan Neptune-Plus Multi-collector Inductively Coupled Plasma Mass Spectrometer (MC-ICP-MS). The purified strontium fractions were diluted with 0.5N HNO_3, adjusting the strontium concentration to 20 µg/L. The reproducibility of the $^{87}Sr/^{86}Sr$ ratio measurements was evaluated through replicate analyses of the NBS 987 standard. An average value 0.710306 ± $10x10^{-6}$ (2σ, n=92) was obtained. Ratios were normalized to the NBS 987 standard value of 0.710245.

2.4 Mineralogical characterization (SEM-EDS and X-ray diffraction)

The mineralogy of a selection (n=7) of surface and core sediment was characterized by scanning electron microscopy (SEM) at Geosciences Paris Sud (GEOPS). Thin sections of powdered material were mounted on a carbon sample-holder, coated with carbon and observed with a Phenom ProX scanning electron microscope using an accelerating voltage of 15keV coupled with an X-ray energy dispersive spectral analyzer for element discrimination.

In addition, core sediment was characterized by X-ray diffraction (XRD) using Cu Kα radiation on powdered core samples. Diffractograms were recorded from 4° to 80° 2θ, under a voltage of 45kV and an intensity of 40mA using a PANalytical X'Pert PRO diffractometer.

These mineralogical analyses were performed to provide information about the potential occurrence of eutrophication processes in the pond and to check for the presence of calcite in sediment samples. Sediment samples were selected depending on $^{87}Sr/^{86}Sr$ ratios and calcium concentrations previously measured to cover their range of variation.

2.5 Source discrimination

Cluster analyses were performed to test the similarity or differences between sediment samples and classify them into individual categories. A hierarchical cluster analysis (HCA) combined with geochemical observations was used to discriminate between sediment samples according to the lithologies of the delineated carbonate and non-carbonate subcatchments (Fig. 1). Clustering analyses were performed with XLstat using the Ward-algorithmic method and the distance between two clusters was defined as the Euclidean distance.

A non-parametric test was used to examine similarities and differences between sediment samples. The Mann-Whitney *U*-test was used to determine the ability of $^{87}Sr/^{86}Sr$ ratios and strontium concentrations to provide a significant discrimination between pond sediment samples at a significance level of $p<0.05$ (Laceby et al., 2015a; Walling, 2005).

2.6 Distribution modeling

A distribution mixing model was used to quantify the relative contributions of sources to sediment (Caitcheon et al., 2012; Foucher et al., 2015; Laceby and Olley, 2014). For ^{137}Cs, a binary mixing model incorporating distributions was used:

$$Ax + B(1 - x) = C \quad \text{(Eq. 2)}$$

where A and B are the modeled distributions of ^{137}Cs in surface and subsurface sources respectively, C is the ^{137}Cs distribution in sediment and *x* is the relative contribution of the surface sources (A). *x* is modeled as a truncated normal distribution ($0 \leq x \leq 1$) with a mixture mean (μ_m) and a standard deviation (σ_m).

As stable isotopes do not mix linearly and are dependent of their elemental concentrations (Laceby et al., 2015b; Phillips and Koch, 2002), a different equation was used to model source concentrations $^{87}Sr/^{86}Sr$ ratio to incorporate their concentration dependency:

$$MMD = ABS\left(\left(E_r - \left(\sum_{s=1}^{m} E_s x_s\right)\right)\Big/ E_r\right) + ABS\left(\left(R_r - \left(\left(\sum_{s=1}^{m} C_s R_s x_s\right)\Big/\left(\sum_{s=1}^{m} C_s R_s\right)\right)\right)\Big/ R_r\right) \quad \text{(Eq. 3)}$$

where E_r is the elemental strontium concentration in the suspended sediment, E_s is the elemental strontium concentration in source (*s*), R_r is the strontium isotopic ratio in the suspended sediment, R_s is the strontium isotopic ratio in sources (s), x_s is the modelled proportional contribution of sources (s); and MMD is the mixing model difference. Absolute values (ABS) are summed in Equation 3.

Non-negative constraints were imposed and normal distributions were modeled for all distributions. Pond and core sediment samples were individually modeled with their analytical error substituted as a standard deviation to model a normal distribution around each of the individual sediment samples (Evrard et al., 2016; Wilkinson et al., 2015).

Source contributions were determined with the Optquest algorithm in Oracle's Crystal Ball Software (see Laceby and Olley (2014)). To determine one optimal source contribution, the μ_m and σ_m for each source's contribution distribution (*x or* x_s) were randomly varied during the equation solving process while minimizing the median difference between both sides of Eq. 2 and the MMD in Eq. 3, and simultaneously solving these equations 2500 times with 2500 random samples (Latin Hypercube - 500 bins) drawn from each sediment and source distribution. This model simulation and solving

process was then repeated 2500 times. The median proportional source contribution (x or x_s) from these 2500 additional simulations is reported as the contribution from each source.

Model uncertainty was determined by summing the modeled standard deviation (σ_m), the median absolute deviation (MAD) of the modeled source contribution and the MAD of the modeled standard deviation for the 2500 model simulations (Laceby et al., 2015a). Results (concentrations and contributions) are presented using the notation ± to express the standard error associated to one sample whereas the mean (μ) and standard deviation (σ) are used for groups of samples.

3 Results

3.1 ^{137}Cs concentrations in source and sediment samples

^{137}Cs activities in channel bank samples ranged from 0.0 to 3.0 Bq kg^{-1} (μ 1.4 Bq kg^{-1}, σ 1 Bq kg^{-1}). In surface soil samples, activities varied between 1.0 and 8.0 Bq kg^{-1} (μ 3.3 Bq kg^{-1}, σ 1.4 Bq kg^{-1}). Surface and subsurface sources were statistically different (p<0.0001). Sediment had higher ^{137}Cs concentrations than their potential source samples with activities varying between 1.2 and 23.1 Bq kg^{-1} (μ 12.6 Bq kg^{-1}, σ 5.5 Bq kg^{-1}) for pond surface sediment and between 10.9 and 16.3 Bq kg^{-1} (μ 13 Bq kg^{-1}, σ 2.4 Bq kg^{-1}) for core sediment. ^{137}Cs concentrations were only considered in sediment from the top layers of the core, between 0 and 16cm of depth (n=5), to avoid disturbances from the input of ^{137}Cs from the Chernobyl accident which had peak activities at 29cm (Foucher et al., 2015) and Fukushima ^{137}Cs fallout inputs were shown to be negligible in France (Evrard et al., 2012).

As pond and core sediment sample concentrations did not plot between the source concentrations, a Th-based particle-size correction was applied (Fig. 2a). After the Th particle size correction, activities in channel bank samples ranged between 0.0 and 1.7 Bq kg^{-1} (μ 1.2 Bq kg^{-1}, σ 0.5 Bq kg^{-1}), between 0.3 and 15.7 Bq kg^{-1} in surface samples (μ 3.8 Bq kg^{-1}, σ 3.0 Bq kg^{-1}), between 0.7 and 4.1 Bq kg^{-1} in pond sediment samples (μ 3.2 Bq kg^{-1}, σ 0.5 Bq kg^{-1}) and between 3.1 and 3.4 Bq kg^{-1} in the upper core sediment samples (μ 3.3 Bq kg^{-1}, σ 0.1 Bq kg^{-1}). The corrected sediment ^{137}Cs concentrations remained within the range of corrected concentrations found in their potential sources (Fig. 2b).

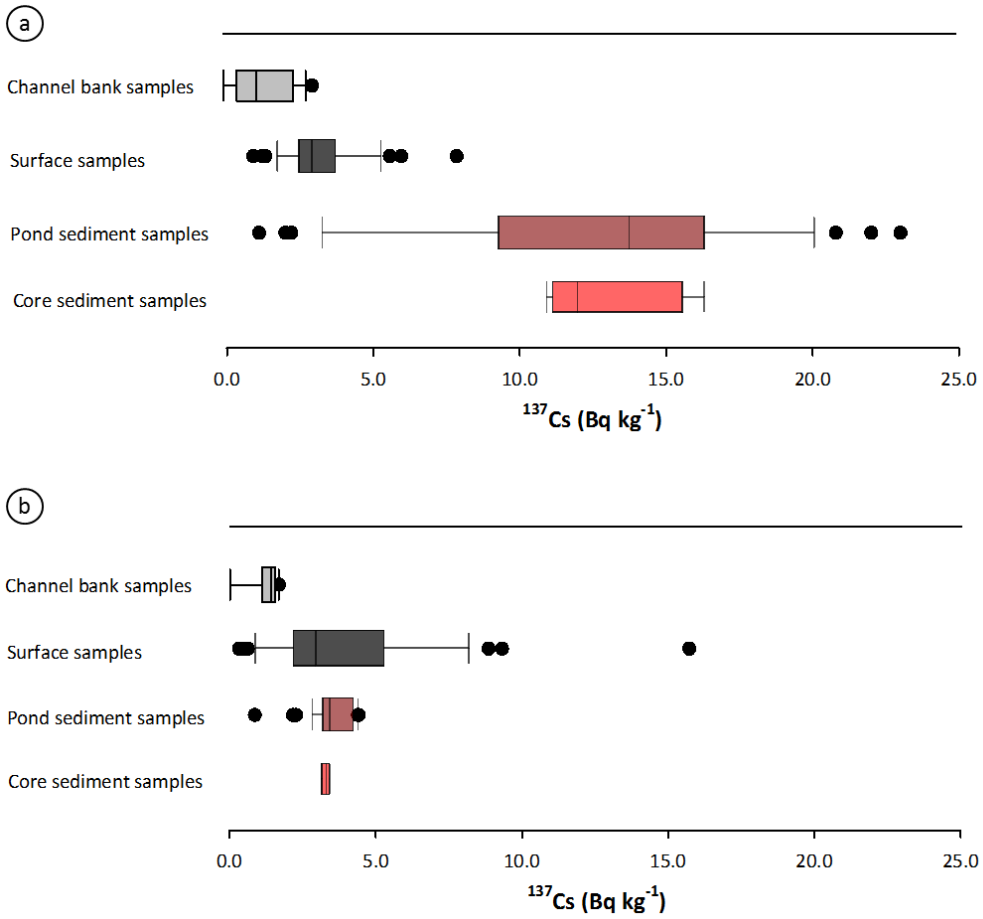

Fig. 2. ^{137}Cs activities (Bq kg^{-1}) in channel bank, soil, pond and core sediment samples before (a) and after (b) the Th particle size correction (bold horizontal line = median, box extent = 25th percentiles, error bars = non-outlier range, black dots = outliers).

3.2 Geochemical discrimination of potential sediment sources

There were large variations in sediment $^{87}Sr/^{86}Sr$ ratios, ranging from 0.710739 to 0.716864 (Table S2) indicating contributions from different lithological sources. The highest values (0.713867 to 0.716761, n=8) were generally observed at the inlet of the stream draining the non-carbonate subcatchment. In contrast, the lowest values (0.711595 to 0.712502, n=6) were found at the inlet of the stream draining the carbonate subcatchment, except for one sample (0.711999) located at the inlet of the non-carbonate subcatchment (Fig. 3a). Intermediate $^{87}Sr/^{86}Sr$ ratios with values between these two end-members (ranging from 0.712151 to 0.714711) characterized sediment collected in downstream sections of the pond (Fig. 3a).

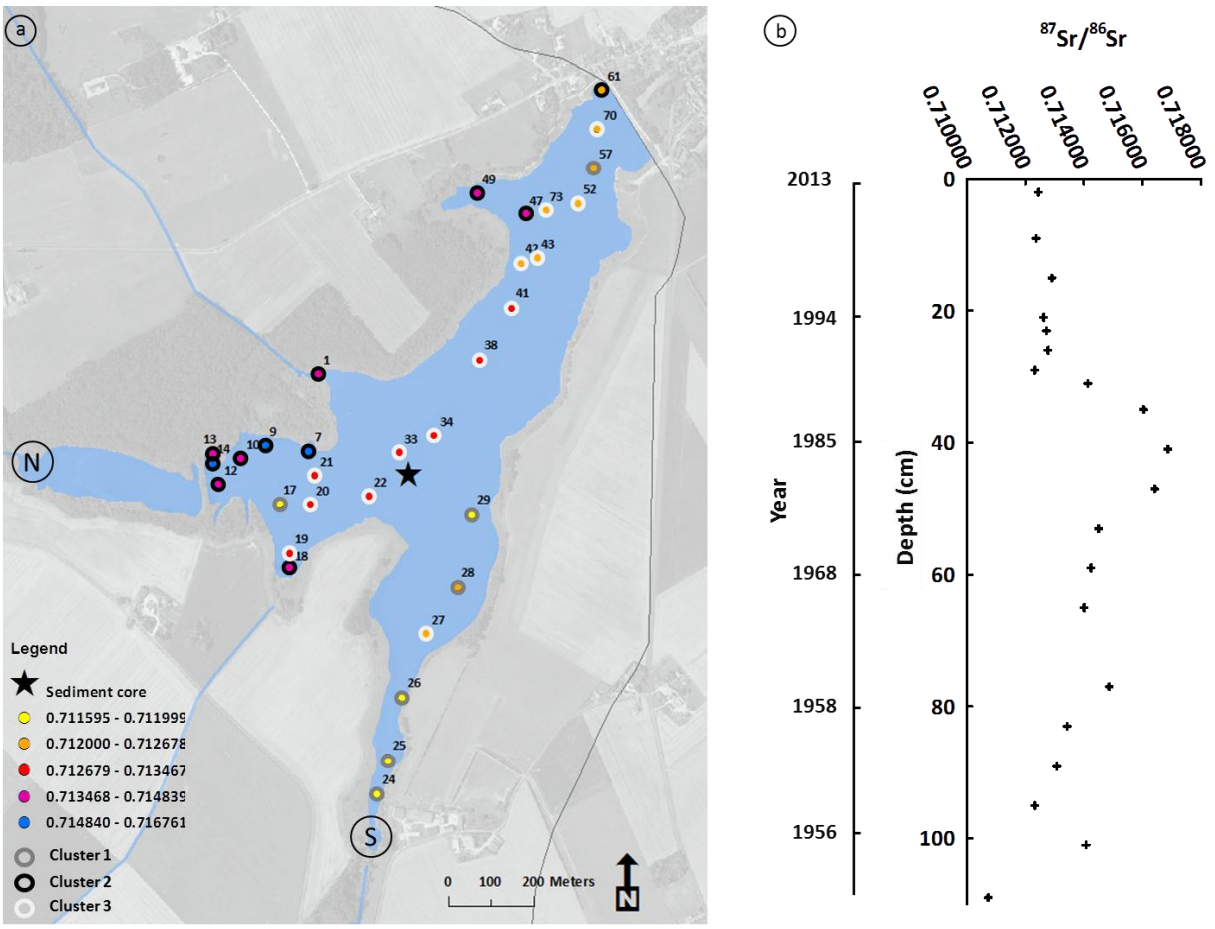

Fig. 3. Spatial (a) and temporal (b) variations of $^{87}Sr/^{86}Sr$ ratios in pond and core sediment samples. N and S correspond to the northern and southern inlets of the main tributaries respectively (a).

A hierarchical cluster analysis (HCA) based on $^{87}Sr/^{86}Sr$ ratios and strontium concentrations was performed to examine potential sources of pond sediment (Fig. S2). Three main groups or clusters were discriminated based on this analysis.

Samples from Cluster 1 (N°24, 25, 26, 28, 29, 17 and 57) are located at the inlet of southern tributaries in the pond with the exception of two samples (N°17 and 57) located at the inlet of the northern tributaries and in the downstream part of the pond. These sediment samples displayed the lowest pond sediment signatures with $^{87}Sr/^{86}Sr$ ratios ranging between 0.711595 and 0.712316.

Samples from Cluster 2 (N°01, 07, 09, 10, 12, 13, 14, 18, 47, 49 and 61) had the highest $^{87}Sr/^{86}Sr$ ratios, with values varying between 0.712466 and 0.716761. They are mainly located in the inlet of the northern tributaries, with the exception of three samples (N°47, 49 and 61) located in downstream areas of the pond.

Cluster 3 (N°19, 20, 21, 22, 27, 33, 34, 38, 41, 43, 52, 70 and 73) is composed of samples located close to the inlet of the northern tributaries, in the middle and in the downstream areas of the pond. One sample (27) located in the inlet of the southern tributaries is likely an outlier. These sediment samples displayed $^{87}Sr/^{86}Sr$ ratios comprised between 0.712502 and 0.713467 and show intermediate values compared to those grouped in Clusters 1 and 3.

When taking into account the location of the sediment samples in the pond, the $^{87}Sr/^{86}Sr$ signatures and the lithologies drained by northern and southern tributaries, sediment samples from Cluster 1 can be defined as a southern/carbonate source (except 17 and 57 samples) whereas sediment samples from Cluster 2 can be referred to as a northern/non-carbonate source (except 47, 49 and 61

samples). The remaining sediment samples (from Cluster 3 and those classified in Clusters 1 and 2 but located in the downstream section of the pond) were hypothesized to be derived from a mixture of sediment originating from the two previously defined end-members. Scatter plots with $^{87}Sr/^{86}Sr$ and elemental ratios (Rb/Sr, Ca/Sr, Mg/Sr, K/Sr, Na/Sr) were also used to confirm the discrimination between these sediment sources (Fig. S3). Therefore, sediment samples collected in the two inlets draining the carbonate and non-carbonate subcatchments were used to characterize the two main potential sources of downstream pond sediment.

In addition to these two main sources, $^{87}Sr/^{86}Sr$ ratios were measured in carbonate rocks, shelly sands and fertilizers. In the carbonate rocks, signatures varied between 0.707968 and 0.708789 while the shelly sand signature reached a value of 0.709538. In fertilizers typically used in this catchment, strontium isotopic ratios varied between 0.707877 and 0.716224. The N fertilizer had the highest value (0.716224). However it was removed from further analysis owing to a very low Sr concentration (0.5 mg kg^{-1}). In P.K and N.P.K fertilizers, Sr ratios varied between 0.707877 and 0.709178 (Table S6). In addition, elevated zinc concentrations were measured in these samples (136 and 184 mg kg^{-1}, respectively, see supplementary material). High zinc concentrations were also observed in surface pond (with concentrations ranging between 67 and 124 mg kg^{-1}) and core sediment (Table S3 and Table S4). In the core, a progressive increase in zinc concentrations was observed from the bottom (47 mg kg^{-1}) to the top (102 mg kg^{-1}).

3.3 Temporal variations of $^{87}Sr/^{86}Sr$ ratios in core sediment samples

In the Louroux sediment core, $^{87}Sr/^{86}Sr$ ratios ranged from 0.710739 to 0.716864 (Fig. 3b). The lowest $^{87}Sr/^{86}Sr$ ratio (0.710739) was observed in 1955, on the bottom of the core. From 1956 to 1976, $^{87}Sr/^{86}Sr$ ratios tended to increase to a maximum of 0.716864. Then, from 1976 to 1986, $^{87}Sr/^{86}Sr$ ratios decreased until they stabilized with values ranging between 0.712318 and 0.712900 from 1986 to 2013 (Fig 3b). Strontium isotopic signatures in core sediment samples have the same range of variations as those observed in pond sediment samples.

3.4 Mineralogical characterization and selective extraction performed on selected core and pond sediment samples

XRD analyses indicated the presence of calcite in all core sediment samples, with contributions varying between 10 and 32% (Table S1). SEM micrographs confirmed the presence of calcite in the sediment samples. The calcite was well precipitated, partially precipitated and potentially associated with clays depending on the samples (Fig. S4f, Fig S4a-b-c-d-g-h and Fig. S4a-b-c-d-i, respectively). Furthermore, silica tubes and diatoms were observed in two core sediment samples (Fig. S4e and g, respectively).

Between 1955 and 1963, the proportion of strontium contained in the exchangeable and carbonate fraction (F1) oscillated between 56 and 73%, the lowest proportion being observed on the bottom of the core. The lowest F1 fraction of the entire sequence (43%) was observed in 1976, before increasing to reach a stable state between 1986 and 2005 with a F1 fraction ranging between 68 and 73% (Fig. 4a).

Between 1955 and 2005, the proportion of calcium contained in the F1 fraction increased from 62% to a maximum of 90%. The highest contributions were observed between 1976 and 2005 (Fig. 4b). $^{87}Sr/^{86}Sr$ ratios measured in the F1 fraction increased from 1955 to 2005, following the same trends

as calcium in this fraction (Fig. 4). The two lowest $^{87}Sr/^{86}Sr$ ratios (0.709216 and 0.709236) were observed in 1955 and 1957. A strong increase was observed from 1957 to 1976, and stable ratios (0.709380 to 0.709395) occurred between 1986 and 2005, when the stabilization of the F1 fraction was observed.

$^{87}Sr/^{86}Sr$ ratios plotted between the signatures of the carbonate rocks, the fertilizers and the shelly sand, suggesting a potential impact of all these sources on the isotopic signature of the core sediment samples (Fig. 5). Sediment sources were thus modeled following a tributary tracing approach (Laceby et al., 2015a; Vale et al., 2016). With this approach, pond sediment samples from inlets of the two main tributaries were modeled as the two main lithological sources (carbonate and non-carbonate) to downstream pond sediment and the sediment core. The potential influence of carbonate rocks, shelly sands, fertilizers, and eutrophication is incorporated within these two tributary sources with this sediment-based sampling approach for surface pond sediment.

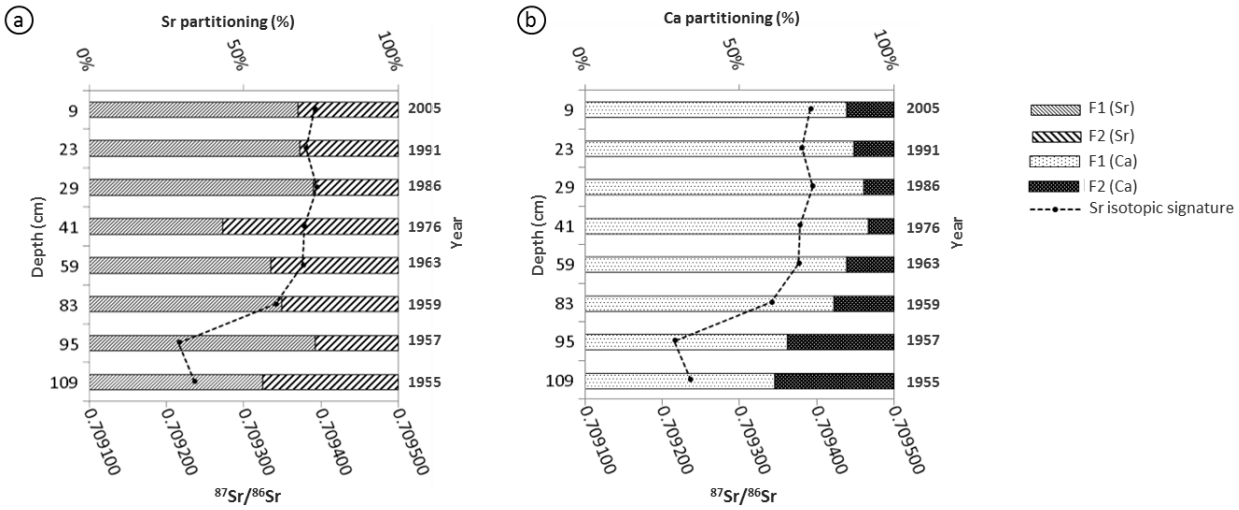

Fig. 4. Strontium (a) and calcium (b) partitioning in core sediment between two defined fractions F1 (exchangeable and carbonate fraction) and F2 (residual fraction) and $^{87}Sr/^{86}Sr$ ratios measured in the fraction F1.

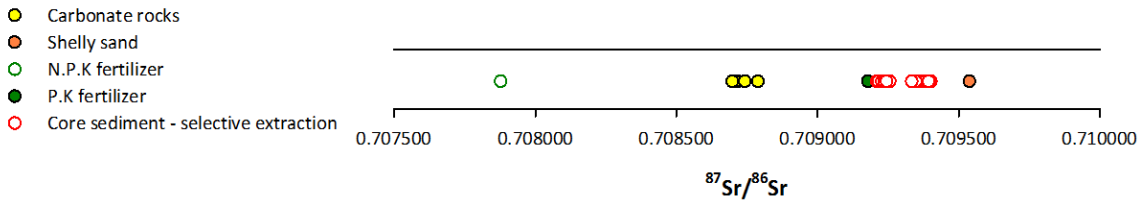

Fig. 5. $^{87}Sr/^{86}Sr$ ratios variations in carbonate rocks, shelly sand, fertilizers and the exchangeable/carbonate fraction of core sediment samples.

3.5 Modeling results

3.5.1 Spatial variations of sediment sources in the pond

Surface sources dominated the supply of sediment to the pond (μ 82%, σ 1%). Surface source contributions varied between 26 ± 1% and 100 ± 4%, and fifteen sediment samples were modeled to be derived exclusively from surface sources (Fig. 6a). Samples characterized by a significant contribution from subsurface sources were mainly located at the inlet of the two main tributaries (the Beaulieu and Grand Bray streams, with contributions of the channel banks varying between 12 ± 1% and 67 ± 1%) or near pond banks in the downstream section of the pond with contributions varying between 7 ± 2% and 75 ± 1%.

Mixing model results using pond sediment samples from the inlet of the two main tributaries as subcatchment sources indicated that the carbonate tributary supplied between 4 ± 1% and 100 ± 1% of downstream sediment in the pond (μ 48, σ 1%) (Fig. 6b). One sediment sample (N°17) located in the inlet of the non-carbonate tributary had a high carbonate contribution of 89 ± 1%. In the central part of the pond, sources contributions were well balanced with the carbonate tributary inputs ranging between 52 ± 1% and 56 ± 1%. In the downstream area of the pond, the carbonate tributary contributions were more variable, with the lowest and the highest contributions observed in this well-mixed section.

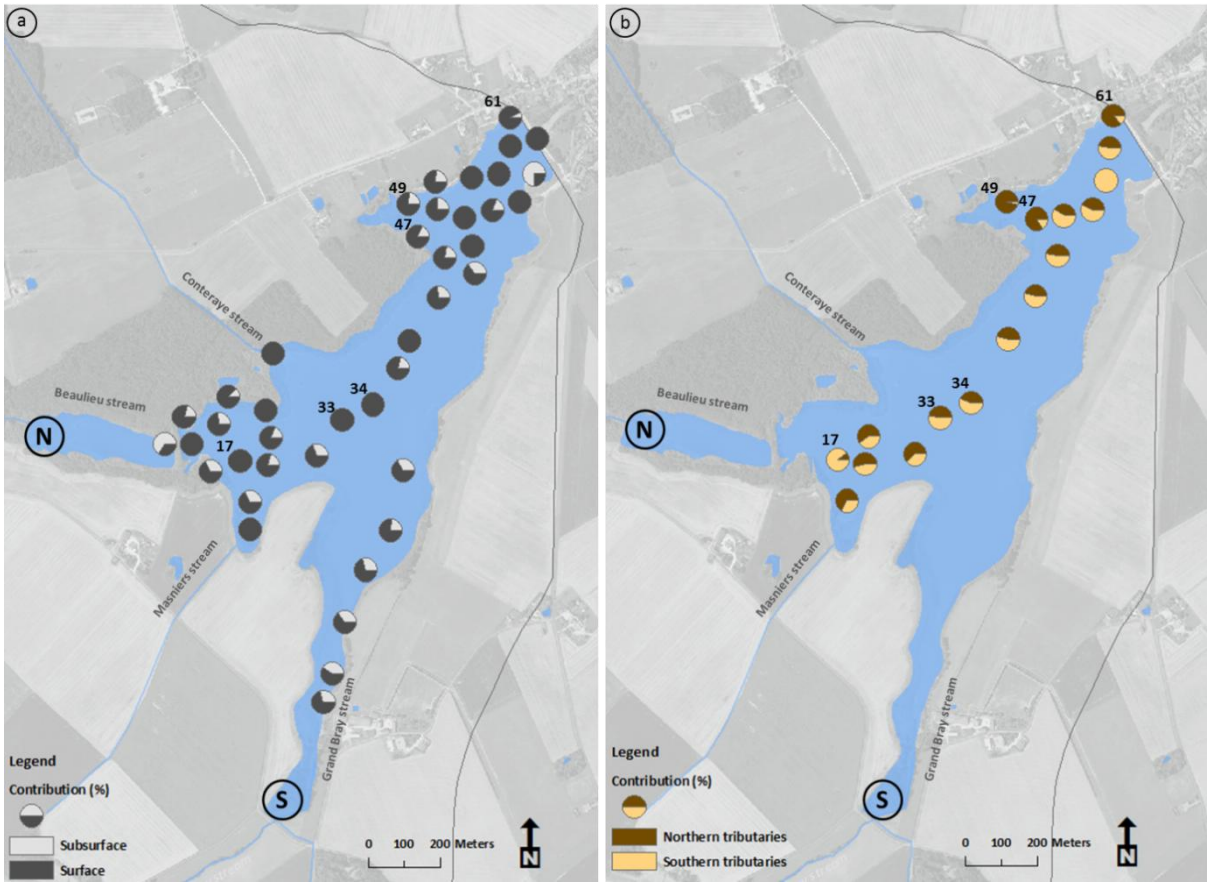

Fig. 6. Contribution of the surface and subsurface sources (a) and of the carbonate and non-carbonate sources (b) to the surface sediment collected in the Louroux pond. N and S correspond to the northern and southern inlets of the main tributaries.

3.5.2 Temporal variation of sediment sources in the core

Modeling results indicate that during the last 17 years, surface sources supplied the majority of core sediment, with a mean contribution of 89 ± 3% (Fig. 7b). Overall, contributions varied between 80 ± 3% and 96 ± 5%. Between 1999 and 2001, a slight increase in the surface source contribution was observed with values increasing from 86 ± 1% to 96 ± 5% before decreasing again between 2009 and 2013 to values between 80 ± 3% and 83 ± 1%. As previously indicated, ^{137}Cs concentrations were only considered in the top 0-16cm to avoid disturbances from the input of ^{137}Cs from the Chernobyl accident recorded at 29cm (Foucher et al., 2015). Accordingly, contributions were not estimated below a depth of 16cm.

Between 1955 and 1957, high variations in sediment spatial sources were observed (Fig. 7a). In 1955, sediment exclusively originated from the southern/carbonate tributary (100 ± 1%). Then, dramatic changes were observed with a dominant contribution from the northern/non-carbonatelcareous tributary (96 ± 4%) in 1956. The main source changed again, with the dominance of the

southern/carbonate tributary (89 ± 2%) in 1957. From 1957 to 1981, the contribution of the northern/non-carbonate tributary progressively increased to a maximum contribution of 100 ± 13%. Then, between 1981 and 1986, these contributions decreased to reach a stable state in the upper part of the core (0-31cm of depth) where the northern/non-carbonate tributary contributed between 30 ± 1% and 47 ± 1% of sediment from 1986 to 2013.

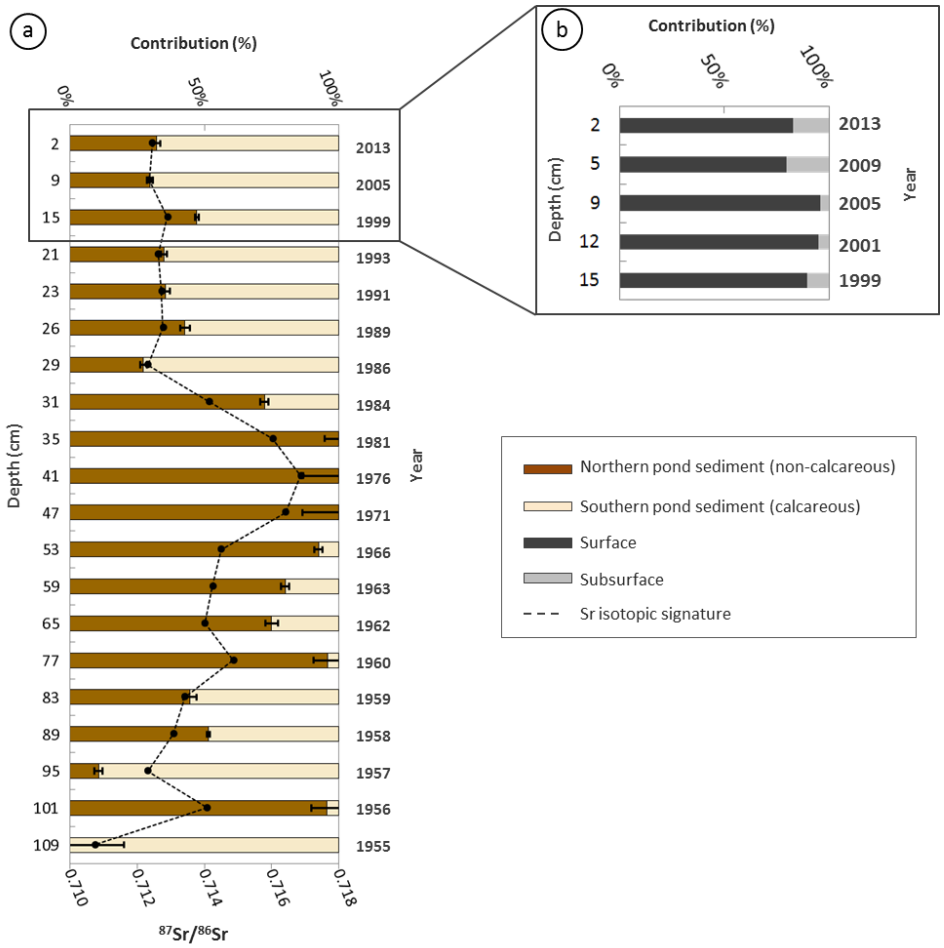

Fig. 7. Evolution of the lithological (a), surface and subsurface (b) sediment sources contributions and $^{87}Sr/^{86}Sr$ ratios along the sediment core (error bars reflect the modelling standard deviation for each sediment sample).

4 Discussion

4.1 Surface and channel bank source contributions

Surface soils were identified as the main source of surface pond sediment. This result is consistent with the observations of Foucher et al. (2015) for suspended sediment collected during flood events upstream of the Louroux pond. They showed that virtually all the sediment originated from the soil surface (μ 98%, σ 2%). However, during low flow periods, they found that suspended sediment transiting the river network had elevated subsurface source contributions (μ 60%, σ 2%) (Foucher et al., 2015). In this current research, subsurface contributions to pond sediment were shown to be significant in areas located in the inlets of the main tributaries close to the pond banks (with contributions ranging between 12 ± 1% and 67 ± 1%). In the rest of the pond, surface sources dominated (μ 86%, σ 1%). The potential erosion of the banks of the pond may also explain the significant contributions of the subsurface source observed near the pond banks and in the

downstream section of the pond, simply owing to their proximity, or possibly smaller tributaries draining into these locations (e.g. N°47, 49).

In the sediment core, there were also subsurface contributions (maximum contribution of 20 ± 3%). These contributions remained stable (μ 11%, σ 3%), indicative of an ongoing channel bank sediment source contribution, though less than what Foucher et al. (2015) modeled for the low-flow conditions in 2013. Overall, channel bank contributions to the pond and core sediment were similar (μ 18%, σ 1% and μ 11%, σ 3% respectively). In fact, the core sediment mean subsoil contribution between 2009 and 2013 (18%) was equivalent to the mean subsoil contribution for the pond sediment. These results suggest that although surface sources dominated sediment supply to the pond during the last seventeen years, channel bank contributions should not be neglected.

4.2 Tributary contributions to pond sediment

Modeling results based on $^{87}Sr/^{86}Sr$ ratios indicate that the southern/carbonate and northern/non-carbonate tributary contributions to pond sediment were nearly equivalent (μ 48%, σ 1% and μ 52%, σ 3% respectively). Over the last seventeen years, both tributaries contributed in stable proportions to sediment sampled in the core (μ 64%, σ 1% for the southern/carbonate tributary).

The southern tributaries drain most of the carbonate substrates that only cover 24% of the catchment surface area and their derived sediment were modeled to contribute more than half of the downstream pond sediment. Therefore, this research implies that the southern/carbonate area supplied disproportionately more sediment to the pond than the northern/non-carbonate area.

One sediment sample (N°17) located in the inlet of the non-carbonate tributary was shown to mainly originate from the carbonate area (89 ± 1%). Field observations indicated that crushed limestone was used to stabilize channel banks in that section of the pond and a mix of sediment and this limestone may have been sampled at that location. Three sediment samples (N°47, 49 and 61) located in the downstream section of the pond were statistically classified as northern/non-carbonate (Cluster 3). Field observations revealed that ephemeral tributaries draining flint clay substrate areas flow into the pond at these locations, which may explain their classification as northern/non-carbonate sediment.

Model results obtained from the core samples demonstrate high variations in lithological sources from 1955 to 2013. The variations are likely related to the spatial evolution of the land consolidation and river design schemes implemented in the catchment since the 1950s. The drastic changes in source contributions observed between 1955 and 1957 could be interpreted as the response to a large-scale phase of land consolidation in 1955 (Foucher et al., 2014). The increasing contribution of the northern/non-carbonate tributary from 1957 to 1981 may be directly related to the implementation of a dense drainage network, the creation of ditches, and the removal of hedges in this northern/non-carbonate area. From 1981 until 1986 the contribution of the carbonate tributary increased and then reached a relatively steady state between 1986 and 2013, with calcareous tributary contributions fluctuating between 53 ± 1% and 70 ± 1%. The Beaulieu pond, located directly upstream of the Louroux pond and currently almost filled sediment, could act as a buffer, reducing the sediment contributions from the northern/non-carbonate tributary to downstream Louroux pond sediment.

$^{87}Sr/^{86}Sr$ ratios, calcium and strontium concentrations (Table S5) were measured in the exchangeable and carbonate fraction of a selection of core sediment samples to provide information on the

biological and chemical processes that may have occurred in the Louroux pond. Results indicated that the carbonate fraction (F1) in the core sediment increased between 1955 and 2005 and had a maximal contribution since 1976. This may be related to higher amounts of carbonates precipitated in the pond during this period, which confirms previous findings showing the occurrence of a progressive eutrophication of the pond. This is confirmed by the presence of algae typical of eutrophic environments and the increase of autochthonous material, with contributions estimated between 44 and 50% (Foucher et al., 2014). These observations are also consistent with the results of XRD and SEM analyses.

Well crystallized calcite was exclusively observed on the bottom of the core (Fig. S4f) during a period that occurred before the implementation of land consolidation programs in the catchment. In contrast, partially precipitated calcite, which is potentially easier to extract, was observed on top of the core, suggesting the occurrence of in situ precipitation. Previous studies conducted in the Loire River (France) observed authigenic calcite precipitation during low flow in summer (Négrel and Grosbois, 1999). In addition, it has been demonstrated that under temperate climates, calcite precipitation can be directly related to inputs of nutrients and thus to primary production (Hamilton et al., 2009). Strontium contributions in the F1 fraction did not follow exactly the same trend as calcium contributions, with a slight shift towards higher ratios in the most recent sediment. This suggests that strontium sources of the carbonate fraction evolved through time and did not exclusively originate from lithological carbonates. Additional sources as fertilizers may potentially explain strontium variations in the carbonate fraction.

4.3 Implications for sediment tracing, catchment management and future studies

The tributary tracing approach may be a useful approach to addressing potential eutrophication, anthropogenic inputs (fertilizers) and in situ precipitation when using $^{87}Sr/^{86}Sr$ ratios for tracing sediment in agricultural catchments. In particular, fertilizers are known to be a major source of contaminants (Zn, Cu, Cd, Pb and Ni) in agricultural soils (Nziguheba and Smolders, 2008) and erosion of these contaminated soils may lead to the deterioration and eutrophication of water bodies (Otero et al., 2005; Vitoria et al., 2004). Furthermore, strontium concentrations may vary between 10 and 4500 mg kg^{-1} in phosphate fertilizers (Otero et al., 2005). Although $^{87}Sr/^{86}Sr$ fractionation in ecological systems is negligible, the redistribution and accumulation of strontium originating from fertilizers in soils may contribute to changes in their isotopic signatures (Borg and Banner, 1996). As an example, Hosono et al. (2007) indicated that 25% of the dissolved Sr was derived from fertilizers in rivers draining a Japanese agricultural catchment. In the Louroux catchment, P.K and N.P.K fertilizers were characterized by high zinc concentrations. Similarly, high Zn concentrations were measured in surface pond sediment and in core sediment since 1983. $^{87}Sr/^{86}Sr$ ratios measured in the mobile fraction (F1) of core sediment were between the signatures of carbonate rocks and shelly sands and the signature of the P.K fertilizers. These results suggest that fertilizers have impacted sediment composition in this catchment since the beginning of the 1980s.

The potential impact of these fertilizers on sediment and source soil properties resulted in the need to adopt a tributary tracing approach in this current research. This approach directly incorporates fertilizers and other potential influences on $^{87}Sr/^{86}Sr$ ratios when tracing the source of downstream sediment in the Louroux Pond. Although the sediment core $^{87}Sr/^{86}Sr$ ratios plotted within the tributary source range, it would be useful for future research to compare 3-5 sediment cores of equivalent length, sampled in each tributary, to sediment cores downstream in order to

580 comprehensively investigate tributary $^{87}Sr/^{86}Sr$ source ratios and variations over an equivalent
581 temporal period.

582 Importantly, these results demonstrate the need to better manage cultivated soils. Land
583 consolidation schemes, modifications in farming practices and in catchment management were
584 shown to have a strong impact on spatial variations of the main sources of sediment. To date,
585 sedimentary archives were mainly collected in lacustrine environments to reconstruct historical
586 sediment fluxes related to environmental changes over longer periods (typically the Holocene
587 period). However, they were mostly collected in mountainous environments (Arnaud et al., 2012;
588 Chapron et al., 2002; Simonneau et al., 2013). Sediment cores were also used to reconstruct
589 concentrations of various contaminants in sediment with time in a large number of rivers of the
590 world (Barra et al., 2001; Bertrand et al., 2013; Elbaz-Poulichet et al., 2011; Rawn et al., 2001). This
591 current approach, combining radionuclide and isotopic geochemical measurements to pond
592 sediment cores, provides important information on sediment source evolution in agricultural lowland
593 catchments in relation to changes in land use and agricultural practices.

594

595 ## 5 Conclusions

596 A targeted fingerprinting approach that combined fallout radionuclides (^{137}Cs), including a thorium-
597 based particle size correction, and strontium isotopic geochemistry ($^{87}Sr/^{86}Sr$) was used to examine
598 spatial and temporal variations of sediment sources in a lowland, drained agricultural catchment. A
599 within-pond tributary tracing approach was developed to mitigate the potential influence of
600 eutrophication, anthropogenic inputs (fertilizers) and in situ precipitation. This research
601 demonstrated the utility of coupling radionuclides and strontium isotopic geochemistry to quantify
602 sediment sources and collecting sediment in pond tributary inlets to use as a source surrogate to
603 trace the origin of sediment sampled downstream.

604 Surface sources dominated the Louroux pond sediment supply (μ 82%, σ 1%). The tributaries draining
605 both the carbonate and the non-carbonate subcatchments contributed approximately half of the
606 surface pond sediment. In contrast, large fluctuations of these tributary contributions were modeled
607 from the analysis of a sediment core. These variations likely reflect the spatial pattern of the land
608 consolidation scheme implemented in this catchment that started in the 1950s.

609 This research demonstrates the utility of using sediment archives to reconstruct the impact of large
610 scale catchment modifications on sediment dynamics. Further analysis of sediment draining
611 agricultural areas should be encouraged to improve our understanding of erosion processes that
612 occurred in these environments. Understanding past impacts of land management on soil erosion
613 and sediment dynamics is fundamental to improving future best management practices in
614 agricultural catchments.

615

616

617

618

Acknowledgements

The authors would like to thank Louise Bordier for technical assistance with ICP-MS measurements, Serge Miska for XRD analyses and Julius Nouet for SEM analyses. This work received financial support from the Loire-Brittany Water Agency (in the framework of the Tracksed and Drastic research projects, under the close supervision of Xavier Bourrain, Jean-Noël Gauthier and Anne Colmar). Marion Le Gall received a PhD fellowship from CEA (Commissariat à l'Energie Atomique et aux Energies Alternatives, France) and DGA (Direction Générale de l'Armement, Ministry of Defense, France).

References

Aberg, G., 1995. The use of natural strontium isotopes as tracers in environmental studies. Water, Air and Soil Pollution, 79: 309-322.

Arnaud, F., Révillon, S., Debret, M., Revel, M., Chapron, E., Jacob, J., Giguet-Covex, C., Poulenard, J., Magny, M., 2012. Lake Bourget regional erosion patterns reconstruction reveals Holocene NW European Alps soil evolution and paleohydrology. Quaternary Science Reviews, 51: 81-92.

Asahara, Y., Ishiguro, H., Tanaka, T., Yamamoto, K., Mimura, K., Minami, M., Yoshida, H., 2006. Application of Sr isotopes to geochemical mapping and provenance analysis: The case of Aichi Prefecture, central Japan. Applied Geochemistry, 21(3): 419-436.

Asahara, Y., Tanaka, T., Kamioka, H., Nishimura, A., Yamazaki, T., 1999. Provenance of the north Pacific sediments and process of source material transport as derived from Rb-Sr isotopic systematics. Chemical Geology, 159: 271-291.

Aubert, D., Stille, P., Probst, A., 2001. REE fractionation during granite weathering and removal by waters and suspended loads: Sr and Nd isotopic evidence. Geochimica et Cosmochimica Acta, 65(3): 387-406.

Ayrault, S., Roy-Barman, M., Le Cloarec, M.F., Priadi, C.R., Bonte, P., Gopel, C., 2012. Lead contamination of the Seine River, France: geochemical implications of a historical perspective. Chemosphere, 87(8): 902-10.

Bakari, S.S., Aagaard, P., Vogt, R.D., Ruden, F., Johansen, I., Vuai, S.A., 2013. Strontium isotopes as tracers for quantifying mixing of groundwater in the alluvial plain of a coastal watershed, south-eastern Tanzania. Journal of Geochemical Exploration, 130: 1-14.

Bakker, M.M., Govers, G., Rounsevell, M.D.A., 2004. The crop productivity–erosion relationship: an analysis based on experimental work. Catena, 57(1): 55-76.

Banowetz, G.M., Whittaker, G.W., Dierkson, K.P., Azevedo, M.D., Kennedy, A.C., Griffith, S.M., Steiner, J.J., 2006. Fatty acide methyl ester analysis to identify sources of soul in surface waters. Journal of Environmental Quality, 35: 133-140.

Barra, R., Cisternas, M., Urrutia, R., Pozo, K., Pacheco, P., Parra, O., Focardi, S., 2001. First report on chlorinated pesticide deposition in a sediment core from a small lake in central Chile. Chemosphere, 45: 749-757.

Bertrand, O., Montargès-Pelletier, E., Mansuy-Huault, L., Losson, B., Faure, P., Michels, R., Pernot, A., Arnaud, F., 2013. A possible terrigenous origin for perylene based on a sedimentary record of a pond (Lorraine, France). Organic Geochemistry, 58: 69-77.

Blum, J.D., Erel, Y., Brown, K., 1994. $^{87}Sr/^{86}Sr$ ratios of Sierra Nevada stream waters: Implications for relative mineral weathering rates. Geochimica et Cosmochimica Acta, 58: 5019-5025.

Boardman, J., 1993. Soil erosion and flooding as a result of a summer thunderstorm in Oxfordshire and Berkshire, May 1993. Applied Geography, 16(1): 21-34.

Boardman, J., Poesen, J., Evans, R., 2003. Socio-economic factors in soil erosion and conservation. Environmental Science & Policy, 6(1): 1-6.

Borg, L.E., Banner, J.L., 1996. Neodymium and strontium isotopic constraints on soil sources in Barbados, West Indies. Geochimica et Cosmochimica Acta, 60(21): 4193-4206.

Brenot, A., Baran, N., Petelet-Giraud, E., Négrel, P., 2008. Interaction between different water bodies in a small catchment in the Paris basin (Brévilles, France): Tracing of multiple Sr sources through Sr isotopes coupled with Mg/Sr and Ca/Sr ratios. Applied Geochemistry, 23(1): 58-75.

Brown, A.G., Carpenter, R.G., Walling, D.E., 2008. Monitoring the fluvial palynomorph load in a lowland temperate catchment and its relationship to suspended sediment and discharge. Hydrobiologia, 607(1): 27-40.

Caitcheon, G.G., Olley, J.M., Pantus, F., Hancock, G., Leslie, C., 2012. The dominant erosion processes supplying fine sediment to three major rivers in tropical Australia, the Daly (NT), Mitchell (Qld) and Flinders (Qld) Rivers. Geomorphology, 151-152: 188-195.

Cerdan, O. et al., 2010. Rates and spatial variations of soil erosion in Europe: A study based on erosion plot data. Geomorphology, 122(1-2): 167-177.

Chapron, E., Desmet, M., De Putter, T., Loutre, M.F., Beck, C., Deconinck, J.F., 2002. Climatic variability in the northwestern Alps, France, as evidenced by 600 years of terrigenous sedimentation in Lake Le Bourget. The Holocene, 12(2): 177-185.

Chartin, C., Evrard, O., Onda, Y., Patin, J., Lefèvre, I., Ottlé, C., Ayrault, S., Lepage, H., Bonté, P., 2013. Tracking the early dispersion of contaminated sediment along rivers draining the Fukushima radioactive pollution plume. Anthropocene, 1: 23-34.

Collins, A.J., Walling, D.E., 2002. Selecting fingerprin properties for discriminating potential suspended sediment sources in river basins. Journal of Hydrology, 261(218-244).

Collins, A.J., Walling, D.E., 2004. Documenting catchment suspended sediment sources: problems, approaches and prospects. Progress in Physical Geography, 28(2): 159-196.

Collins, A.L., Zhang, Y., McChesney, D., Walling, D.E., Haley, S.M., Smith, P., 2012. Sediment source tracing in a lowland agricultural catchment in southern England using a modified procedure combining statistical analysis and numerical modelling. Science of the Total Environment, 414: 301-17.

Davis, C.M., Fox, J.F., 2009. Sediment fingerprinting: review of the method and future improvemments for allocating nonpoint source pollution. Journal of Environmental Engineering, 135: 490-504.

Devlin, M.J., Barry, J., Mills, D.K., Gowen, R.J., Foden, J., Sivyer, D., Tett, P., 2008. Relationships between suspended particulate material, light attenuation and Secchi depth in UK marine waters. Estuarine, Coastal and Shelf Science, 79(3): 429-439.

Dotterweich, M., 2013. The history of human-induced soil erosion: Geomorphic legacies, early descriptions and research, and the development of soil conservation—A global synopsis. Geomorphology, 201: 1-34.

Douglas, G., Palmer, M., Caitcheon, G.G., 2003. The provenance of sediments in Moreton Bay, Australia: a synthesis of major, trace element and Sr-Nd-Pb isotopic geochemistry, modelling and landscape analysis. Hydrobiologia, 494: 145-151.

Douglas, T.A., Gray, C.M., Hart, B.T., Beckett, R., 1995. A strontium isotopic investigation of the origin of suspended particulate matter (SPM) in the Murrat-Darling River system, Australia. Geochimica et Cosmochimica Acta, 59(18): 3799-3815.

Eikenberg, J., Tricca, A., Vezzu, G., Stille, P., Bajo, S., Ruethi, M., 2001. $^{228}Ra/^{226}Ra/^{224}Ra$ and $^{87}Sr/^{86}Sr$ isotope relationships for determining interactions between ground and river water in the upper Rhine valley. Journal of Environmental Radioactivity, 54: 133-162.

Elbaz-Poulichet, F., Dezileau, L., Freydier, R., Cossa, D., Sabatier, P., 2011. A 3500-Year Record of Hg and Pb Contamination in a Mediterranean Sedimentary Archive (The Pierre Blanche Lagoon, France). Environmental Science & Technology, 45(20): 8642-8647.

Evrard, O., Bielders, C.L., Vandaele, K., van Wesemael, B., 2007. Spatial and temporal variation of muddy floods in central Belgium, off-site impacts and potential control measures. Catena, 70(3): 443-454.

Evrard, O., Laceby, J.P., Huon, S., Lefèvre, I., Sengtaheuanghoung, O., Ribolzi, O., 2016. Combining multiple fallout radionuclides (^{137}Cs, ^{7}Be, $^{210}Pb_{xs}$) to investigate temporal sediment source

dynamics in tropical, ephemeral riverine systems. Journal of Soils and Sediments, 16(3): 1130-1144.
Evrard, O., Navratil, O., Ayrault, S., Ahmadi, M., Némery, J., Legout, C., Lefèvre, I., Poirel, A., Bonté, P., Esteves, M., 2011. Combining suspended sediment monitoring and fingerprinting to determine the spatial origin of fine sediment in a mountainous river catchment. Earth Surface Processes and Landforms, 36(8): 1072-1089.
Evrard, O., Van Beek, P., Gateuille, D., Pont, V., Lefevre, I., Lansard, B., Bonte, P., 2012. Evidence of the radioactive fallout in France due to the Fukushima nuclear accident. Journal of Environmental Radioactivity, 114: 54-60.
Faure, G., 1986. Principles of Isotopic Geology. Wiley, New York.
Foucher, A., Laceby, P.J., Salvador-Blanes, S., Evrard, O., Le Gall, M., Lefèvre, I., Cerdan, O., Rajkumar, V., Desmet, M., 2015. Quantifying the dominant sources of sediment in a drained lowland agricultural catchment: The application of a thorium-based particle size correction in sediment fingerprinting. Geomorphology, 250: 271-281.
Foucher, A., Salvador-Blanes, S., Evrard, O., Simonneau, A., Chapron, E., Courp, T., Cerdan, O., Lefèvre, I., Adriaensen, H., Lecompte, F., Desmet, M., 2014. Increase in soil erosion after agricultural intensification: Evidence from a lowland basin in France. Anthropocene, 7: 30-41.
Froger, D., Moulin, J., Servant, J., 1994. Les terres Gatines, Boischaud-Nord, Pays-Fort, Touraine-Berry. Typologie des sols. Chambres d'agriculture du Cher, de l'Indre, de l'Indre et Loire et du Loire et Cher.
Gaillardet, J., Dupré, B., Allègre, C.J., Négrel, P., 1997. Chemical and physical denudation in the Amazon River Basin. Chemical Geology, 142: 141-173.
García-Ruiz, J.M., 2010. The effects of land uses on soil erosion in Spain: A review. Catena, 81(1): 1-11.
Gateuille, D., Evrard, O., Lefevre, I., Moreau-Guigon, E., Alliot, F., Chevreuil, M., Mouchel, J.M., 2014. Mass balance and decontamination times of Polycyclic Aromatic Hydrocarbons in rural nested catchments of an early industrialized region (Seine River basin, France). Science of the Total Environment, 470-471: 608-17.
Goldstein, S.J., Jacobsen, S.B., 1988. Nd and Sr isotopic systematics of river water suspended material: implications for crustal evolution. Earth and Planetary Science Letters, 87: 249-265.
Graustein, W.C., 1989. $^{87}Sr/^{86}Sr$ ratios measure the sources and flow of strontium in terrestrial environment. In: Springer, N.-Y. (Ed.), Stable Isotopes in Ecological Research, pp. 491-512.
Grosbois, C., Négrel, P., Fouillac, C., Grimaud, D., 2000. Dissolved load of the Loire River: chemical and isotopic characterization. Chemical Geology, 170: 179-201.
Guzmán, G., Quinton, J.N., Nearing, M.A., Mabit, L., Gómez, J.A., 2013. Sediment tracers in water erosion studies: current approaches and challenges. Journal of Soils and Sediments, 13(4): 816-833.
Haddadchi, A., Ryder, D.S., Evrard, O., Olley, J., 2013. Sediment fingerprinting in fluvial systems: review of tracers, sediment sources and mixing models. International Journal of Sediment Research, 28(4): 560-578.
Hamilton, S.K., Bruesewitz, D.A., Horst, G.P., Weed, D.B., Sarnelle, O., 2009. Biogenic calcite–phosphorus precipitation as a negative feedback to lake eutrophication. Canadian Journal of Fisheries and Aquatic Sciences, 66(2): 343-350.
Hatfield, R.G., Maher, B.A., 2009. Fingerprinting upland sediment sources: particle size-specific magnetic linkages between soils, lake sediments and suspended sediments. Earth Surface Processes and Landforms, 34(10): 1359-1373.
Hatfield, R.G., Maher, B.A., Pates, J.M., Barker, P.A., 2008. Sediment dynamics in an upland temperate catchment: changing sediment sources, rates and deposition. Journal of Paleolimnology, 40: 1143-1158.
He, Q., Walling, D.E., 1996. Interpreting particle size effects in the adsorption of ^{137}Cs and unsupported ^{210}Pb by mineral soils and sediment. Journal of Environmental Radioactivity, 30(2): 117-137.

Horowitz, A.J., 2008. Determining annual suspended sediment and sediment-associated trace element and nutrient fluxes. Science of the Total Environment, 400(1-3): 315-43.

Hosono, T., Nakano, T., Igeta, A., Tayasu, I., Tanaka, T., Yachi, S., 2007. Impact of fertilizer on a small watershed of Lake Biwa: use of sulfur and strontium isotopes in environmental diagnosis. Science of the Total Environment, 384(1-3): 342-54.

Jørgensen, N.O., Andersen, M.S., Engesgaard, P., 2008. Investigation of a dynamic seawater intrusion event using strontium isotopes ($^{87}Sr/^{86}Sr$). Journal of Hydrology, 348(3-4): 257-269.

Koiter, A.J., Owens, P.N., Petticrew, E.L., Lobb, D.A., 2013. The behavioural characteristics of sediment properties and their implications for sediment fingerprinting as an approach for identifying sediment sources in river basins. Earth-Science Reviews, 125: 24-42.

Laceby, J.P., McMahon, J., Evrard, O., Olley, J., 2015a. A comparison of geological and statistical approaches to element selection for sediment fingerprinting. Journal of Soils and Sediments, 15(10): 2117-2131.

Laceby, J.P., Olley, J., 2014. An examination of geochemical modelling approaches to tracing sediment sources incorporating distribution mixing and elemental correlations. Hydrological Processes, 29(6): 1669-1685.

Laceby, J.P., Olley, J., Pietsch, T.J., Sheldon, F., Bunn, S.E., 2015b. Identifying subsoil sediment sources with carbon and nitrogen stable isotope ratios. Hydrological Processes, 29(8): 1956-1971.

Le Bissonnais, Y., Cerdan, O., Lecomte, V., Benkhadra, H., Souchère, V., Martin, P., 2005. Variability of soil surface characteristics influencing runoff and interrill erosion. Catena, 62(2-3): 111-124.

Le Gall, M., Evrard, O., Thil, F., Foucher, A., Laceby, J.P., Salvador-Blanes, S., Ayrault, S., under review. Examining suspended sediment sources and dynamics during flood events in a drained catchment using radiogenic strontium isotope ratios ($^{87}Sr/^{86}Sr$).

Mabit, L., Benmansour, M., Walling, D.E., 2008. Comparative advantages and limitations of the fallout radionuclides (137)Cs, (210)Pb(ex) and (7)Be for assessing soil erosion and sedimentation. Journal of Environmental Radioactivity, 99(12): 1799-807.

Martínez-Carreras, N., Udelhoven, T., Krein, A., Gallart, F., Iffly, J.F., Ziebel, J., Hoffmann, L., Pfister, L., Walling, D.E., 2010. The use of sediment colour measured by diffuse reflectance spectrometry to determine sediment sources: Application to the Attert River catchment (Luxembourg). Journal of Hydrology, 382(1-4): 49-63.

Motha, J.A., Wallbrink, P.J., Hairsine, P.B., Grayson, R.B., 2003. Determining the sources of suspended sediment in a forested catchment in southeastern Australia. Water Resources Research, 39(3): 39-1059.

Négrel, P., Grosbois, C., 1999. Changes in chemical and $^{87}Sr/^{86}Sr$ signature distribution patterns of suspended matter and bed sediments in the upper Loire river basin (France). Chemical Geology, 156: 231-249.

Négrel, P., Roy, S., 1998. Chemistry of rainwater in the Massif Central (France): a strontium isotope and major element study. Applied Geochemistry, 13(8): 941-952.

Nosrati, K., Govers, G., Ahmadi, H., Sharifi, F., Amoozegar, M.A., Merckx, R., Vanmaercke, M., 2011. An exploratory study on the use of enzyme activities as sediment tracers: biochemical fingerprints? International Journal of Sediment Research, 26(2): 136-151.

Nziguheba, G., Smolders, E., 2008. Inputs of trace elements in agricultural soils via phosphate fertilizers in European countries. Science of the Total Environment, 390(1): 53-7.

Olley, J., Brooks, A., Spencer, J., Pietsch, T., Borombovits, D., 2013. Subsoil erosion dominates the supply of fine sediment to rivers draining into Princess Charlotte Bay, Australia. Journal of Environmental Radioactivity, 124: 121-9.

Olley, J.M., Murray, A.S., Mackenzie, D.H., Edwards, K., 1993. Identifying sediment sources in a gullied catchment using natural and anthropogenic radioactivity. Water Resources Research, 29(4): 1037-1043.

Otero, N., Vitòria, L., Soler, A., Canals, A., 2005. Fertiliser characterisation: Major, trace and rare earth elements. Applied Geochemistry, 20(8): 1473-1488.

Owens, P.N., Batalla, R.J., Collins, A.J., Gomez, B., Hicks, D.M., Horowitz, A.J., Kondolf, G.M., Marden, M., Page, M.J., Peacock, D.H., Petticrew, E.L., Salomons, W., Trustrum, N.A., 2005. Fine-grained sediment in river systems: environmental significance and management issues. River Research and Applications, 21(7): 693-717.

Owens, P.N., Walling, D.E., 2002. Changes in sediment sources and floodplain deposition rates in the catchment of the River Tweed, Scotland, over the last 100 years: the impact of climate and land use change. Earth Surface Processes and Landforms, 27(4): 403-423.

Pande, K., Sarin, M.M., Trivedi, J.R., Krishnaswami, S., Sharma, K.K., 1994. The Indus river system (India-Pakistan): Major-ion chemistry, uranium and strontium isotopes. Chemical Geology, 116: 245-259.

Petelet-Giraud, E., Négrel, P., Gourcy, L., Schmidt, C., Schirmer, M., 2007. Geochemical and isotopic constraints on groundwater-surface water interactions in a highly anthropized site. The Wolfen/Bitterfeld megasite (Mulde subcatchment, Germany). Environmental Pollution, 148(3): 707-17.

Phillips, D.L., Koch, P.L., 2002. Incorporating concentration dependence in stable isotope mixing models. Oecologia, 130(1): 114-125.

Poulenard, J., Legout, C., Némery, J., Bramorski, J., Navratil, O., Douchin, A., Fanget, B., Perrette, Y., Evrard, O., Esteves, M., 2012. Tracing sediment sources during floods using Diffuse Reflectance Infrared Fourier Transform Spectrometry (DRIFTS): A case study in a highly erosive mountainous catchment (Southern French Alps). Journal of Hydrology, 414-415: 452-462.

Pueyo, M., Rauret, G., Lück, D., Yli-Halla, M., Muntau, H., Quevauviller, P., López-Sánchez, J.F., 2001. Certification of the extractable contents of Cd, Cr, Cu, Ni, Pb and Zn in a freshwater sediment following a collaboratively tested and optimised three-step sequential extraction procedure. Journal of Environmental Monitoring, 3: 243-250.

Rasplus, L., Macaire, J.J., Alcaydé, G., 1982. Carte géologique de Bléré au 1:5000, Editions BRGM.

Rauret, G., López-Sánchez, J.F., Sahuquillo, A., Rubio, R., Davidson, C., Ure, A., Quevauviller, P., 1999. Improvement of the BCR three step sequential extraction procedure prior to the certification of new sediment and soil reference materials. Journal of Environmental Monitoring, 1(1): 57-61.

Rawn, D.F.K., Lockhart, W.L., Wilkinson, P., Savoie, D.A., Rosenberg, G.B., Muir, D.C.G., 2001. Historical contamination of Yukon Lake sediments by PCBs and organochlorine pesticides : influence of local sources and watershed characteristics. Science of the Total Environment, 280: 17-37.

Russell, M.A., Walling, D.E., Hodgkinson, R.A., 2001. Suspended sediment sources in two small lowland agricultural catchments in the UK. Journal of Hydrology, 252: 1-24.

Simonneau, A. et al., 2013. Holocene land-use evolution and associated soil erosion in the French Prealps inferred from Lake Paladru sediments and archaeological evidences. Journal of Archaeological Science, 40(4): 1636-1645.

Smith, H.G., Dragovich, D., 2008. Improving precision in sediment source and erosion process distinction in an upland catchment, south-eastern Australia. Catena, 72(1): 191-203.

Smith, J.P., Bullen, T.D., Brabander, D.J., Olsen, C.R., 2009. Strontium isotope record of seasonal scale variations in sediment sources and accumulation in low-energy, subtidal areas of the lower Hudson River estuary. Chemical Geology, 264(1-4): 375-384.

Sogon, S., Penven, M.-J., Bonte, P., Muxart, T., 1999. Estimation of sediment yield and soil loss using suspended sediment load and 137Cs measurements on agricultural land, Brie Plateau, France. Hydrobiologia, 410: 251-261.

Tiecher, T., Caner, L., Minella, J.P.G., Bender, M.A., dos Santos, D.R., 2015. Tracing sediment sources in a subtropical rural catchment of southern Brazil by using geochemical tracers and near-infrared spectroscopy. Soil and Tillage Research.

Vale, S.S., Fuller, I.C., Procter, J.N., Basher, L.R., Smith, I.E., 2016. Application of a confluence-based sediment-fingerprinting approach to a dynamic sedimentary catchment, New Zealand. Hydrological Processes, 30(5): 812-829.

Valentin, C., Poesen, J., Li, Y., 2005. Gully erosion: Impacts, factors and control. Catena, 63(2-3): 132-153.

Viers, J., Dupré, B., Braun, J.J., Deberdt, S., Angeletti, B., Ndam Ngoupayou, J., Michard, A., 2000. Major and trace element abundances, and strontium isotopes in the Nyong basin rivers (Cameroon): constraints on chemical weathering processes and elements transport mechanisms in humid tropical environments. Chemical Geology, 169(1-2): 211-241.

Vitoria, L., Otero, N., Soler, A., Canals, A., 2004. Fertilizer characterisation: Isotopic data (N, S, O, C, and Sr). Envionmental Science & Technology, 38: 3254-3262.

Vörösmarty, C.J., Meybeck, M., Fekete, B., Sharma, K., Green, P., Syvitski, J.P.M., 2003. Anthropogenic sediment retention: major global impact from registered river impoundments. Global and Planetary Change, 39(1-2): 169-190.

Walling, D.E., 2005. Tracing suspended sediment sources in catchments and river systems. Science of the Total Environment, 344(1-3): 159-84.

Walling, D.E., Collins, A.L., Stroud, R.W., 2008. Tracing suspended sediment and particulate phosphorus sources in catchments. Journal of Hydrology, 350(3-4): 274-289.

Walling, D.E., Owens, P.N., Waterfall, B.D., Graham, J.L., Wass, P.D., 2000. The particle size characteristics of fluvial suspended sediment in the Humber and Tweed catchments, UK. Science of the Total Environment, 251/252: 205-222.

Walling, D.E., Russell, M.A., Hodgkinson, R.A., Zhang, Y., 2002. Establishing sediment budgets for two small lowland agricultural catchments in the UK. Catena, 47: 323-353.

Wasson, R.J., Caitcheon, G.G., Murray, A.S., McCulloch, M., Quade, J., 2002. Sourcing sediment using multiple tracers in the catchment of Lake Argyle, Northwestern Australia. Environmental Management, 29(5): 634-646.

Wilkinson, S.N., Olley, J.M., Furuichi, T., Burton, J., Kinsey-Henderson, A.E., 2015. Sediment source tracing with stratified sampling and weightings based on spatial gradients in soil erosion. Journal of Soils and Sediments, 15(10): 2038-2051.

Yasuda, T., Asahara, Y., Ichikawa, R., Nakatsuka, T., Minami, H., Nagao, S., 2014. Distribution and transport processes of lithogenic material from the Amur River revealed by the Sr and Nd isotope ratios of sediments from the Sea of Okhotsk. Progress in Oceanography, 126: 155-167.

Supplementary material

Material and methods: additional information

Mineralization and selective extraction of the "exchangeable and carbonate" fraction

Approximately 100 mg of source and sediment material were dissolved by the successive addition of 3 mL HF (47-51%) and 3 mL $HClO_4$ (65-71%) at 150°C and 3.75 mL HCl (34-37%) and 1.25 mL HNO_3 (67%) at 110°C in closed Teflon vessels on hot-plates. Next, the samples were re-suspended three times in 2 mL of HNO_3 (67%) and then diluted in 50 mL of ultrapure water (Milli-Q). Between each step, solutions were evaporated to dryness and ultrapure reagents were used (Normatom grade, VWR, France for HNO_3, and "Trace Metal Grade", Fisher Chemical, France for HF, $HClO_4$ and HCl). A reference material (IAEA lake sediment SL1) and a chemical blank were analyzed to check the chemical mineralization efficiency for each set of digestions.

A two-step procedure was applied to carbonate rocks. To clean the surface, approximately 125 mg of powdered material was leached in 10 mL of HNO_3 0.5N. The solution was then centrifuged; the supernatant solution taken away and the residue dissolved twice again, following the same procedure. The solid residue was dissolved by the successive addition of 0.25 mL HNO_3 (67%) and 1.35 mL HCl (34-37%) at 110°C and 0.5 mL HF (47-51%) and 0.5 mL $HClO_4$ (65-71%) at 150°C in Teflon vessels on hot plates. Samples were evaporated to dryness between 110°C and 150°C. Samples were finally resuspended in 0.5 mL of HNO_3 and diluted with the supernatant solution in 50 mL of ultrapure water (Milli-Q).

For fertilizers, 100 mg of material (N, N.P.K and P.K) were dissolved in 5 mL of HNO_3 5N to extract the maximum amount of phosphorous and to minimize subsequent precipitation of insoluble compounds. The solution was then centrifuged, the supernatant solution taken away and the residue dissolved again twice, following the same procedure. Residues were then digested in Teflon vessels on hot plates with a 1.5 mL HF (47-51%) and 1.5 mL $HClO_4$ (65-71%) mixture at 180°C for 2 days and evaporated to dryness at 150°C. The supernatant was then added to the residue and evaporated to dryness at 150°C. Samples were finally resuspended three times in 1 mL of HNO_3 and diluted to 50 mL with ultrapure water (Milli-Q).

Strontium purification

A strontium specific resin was used (SR Resin, 100-150 µm, TrisKem International) and packed on lab-made polyethylene microcolumns. The resin was previously conditioned using HCl 1N and HCl 3N and rinsed with HNO_3 3N and ultrapure water (Milli-Q). A pure Sr fraction was separated from the digestion solution using HNO_3 3N and ultrapure water (Milli-Q). Strontium recovery and efficiency of purification were determined by comparing the strontium, and calcium concentrations in the original solution (after bulk mineralization) and in the eluted strontium fraction. More than 90% of the calcium was eliminated after the chemical extraction.

Detailed geological map of the Louroux catchment (Froger et al., 1994; Rasplus et al., 1982)

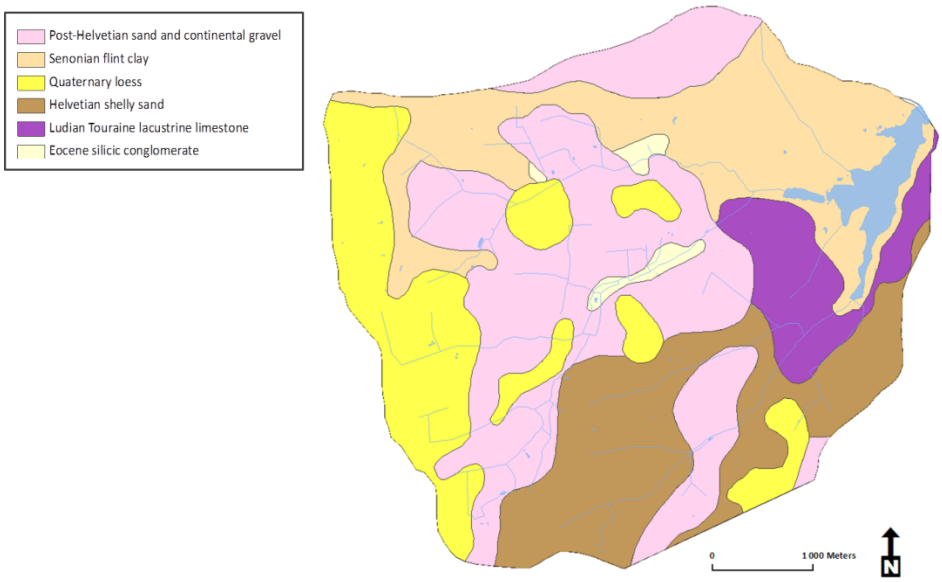

Fig. S1. Detailed lithological map of the Louroux catchment.

Geochemical discrimination of pond and core sediment

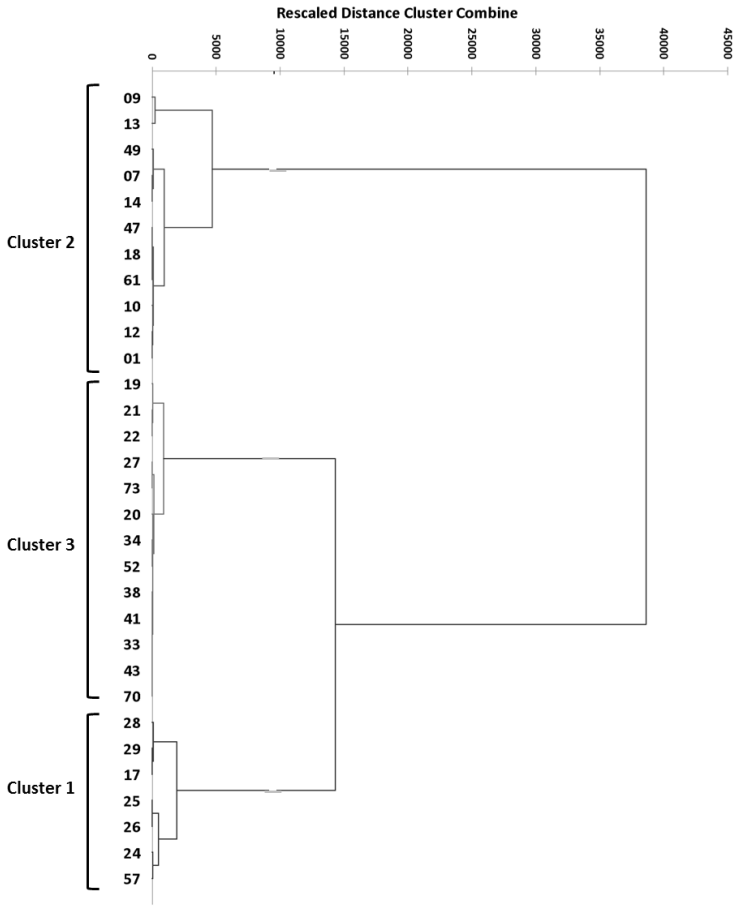

Fig. S2. Dendogram of the hierarchical cluser analysis based on $^{87}Sr/^{86}Sr$ ratios and strontium concentrations.

$^{87}Sr/^{86}Sr$ and elemental ratios (Rb/Sr, Ca/Sr, Mg/Sr, K/Sr, Na/Sr) were used to confirm the statistical discrimination between pond sediment sources (Fig. S2). Pond sediment samples with low $^{87}Sr/^{86}Sr$,

Rb/Sr, Mg/Sr, K/Sr, Na/Sr values and high Ca/Sr ratios correspond to the sediment discriminated as southern/carbonate pond sediment samples. They are enriched in Ca and Sr, suggesting a carbonate origin. On the contrary, pond sediment samples with high $^{87}Sr/^{86}Sr$, Rb/Sr, Mg/Sr, K/Sr, Na/Sr values and low Ca/Sr ratios correspond to sediment discriminated as northern/non-carbonate pond sediment samples. They are depleted in Ca and Sr, but enriched in Rb, which suggests a more siliceous origin. The remaining pond sediment samples are well scattered between these southern/carbonate and northern/non-carbonate pond sediment samples. Accordingly, these observations are consistent with the statistical analysis performed in the main text of the manuscript and indicate that pond sediment originate from a mix between two different lithological sources. The Mann-Whitney U-test confirmed the ability of $^{87}Sr/^{86}Sr$ ratios and Sr concentrations to discriminate between the southern/carbonate and northern/non-carbonate sediment sources (MW p=0.001). Furthermore, $^{87}Sr/^{86}Sr$ signatures from core sediment samples were comprised in the range of values measured in pond sediment samples. Therefore, southern/carbonate and northern/non-carbonate pond sediment samples will be used as sediment sources for the core in mixing models.

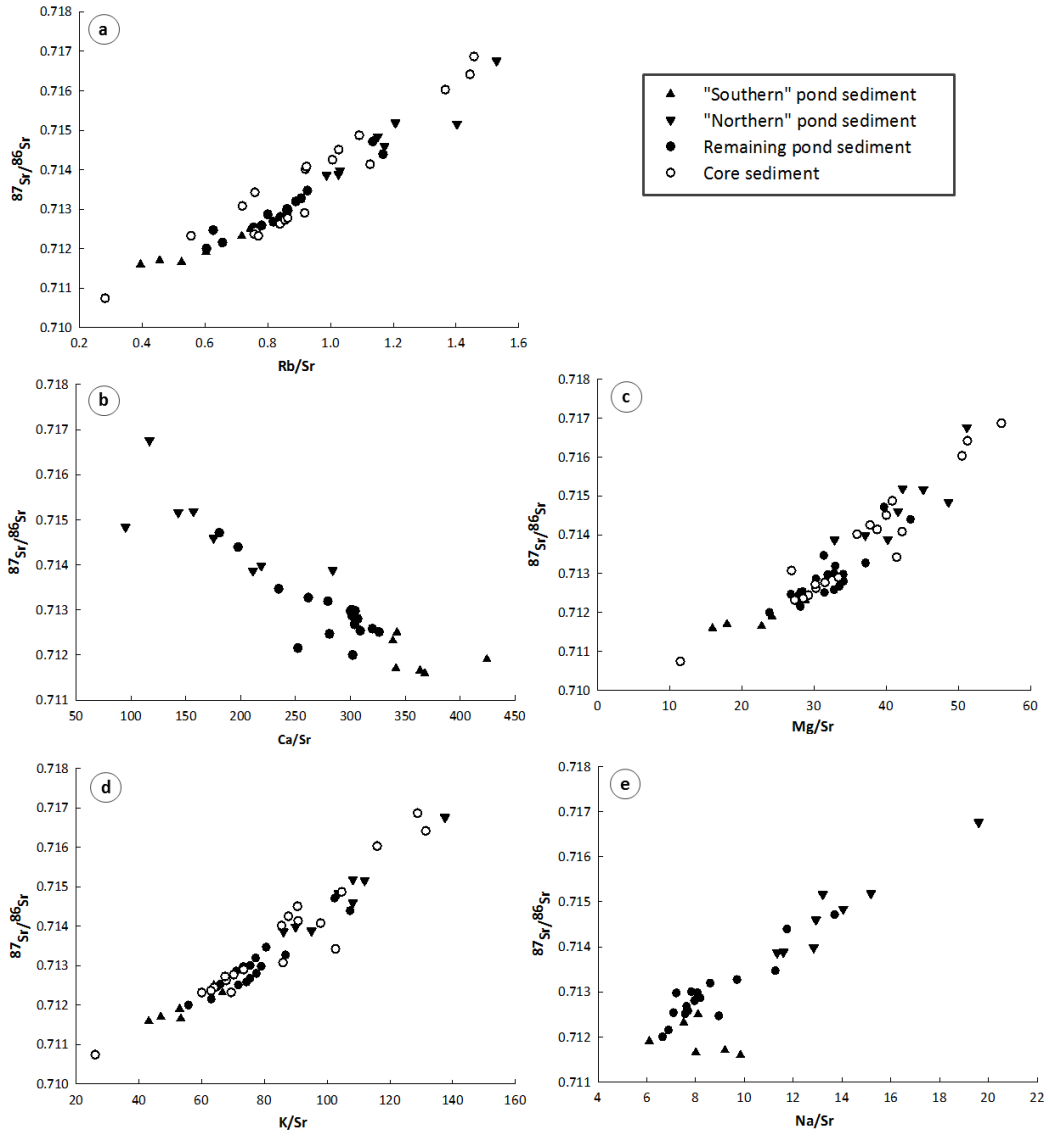

Fig. S3. Scatter plot of $^{87}Sr/^{86}Sr$ vs Rb/Sr (a), Ca/Sr (b), Mg/Sr (c), K/Sr (d) and Na/Sr (e).

Table S1. Semi-quantitative XRD analyses in core sediment (n=4).

Sample	Calcite (%)	Quartz (%)	Other minerals (%)
CO 09-11cm	32	27	41
CO 59-61cm	11	45	44
CO 83-85cm	10	34	56
CO 95-97cm	19	60	21

SEM analysis

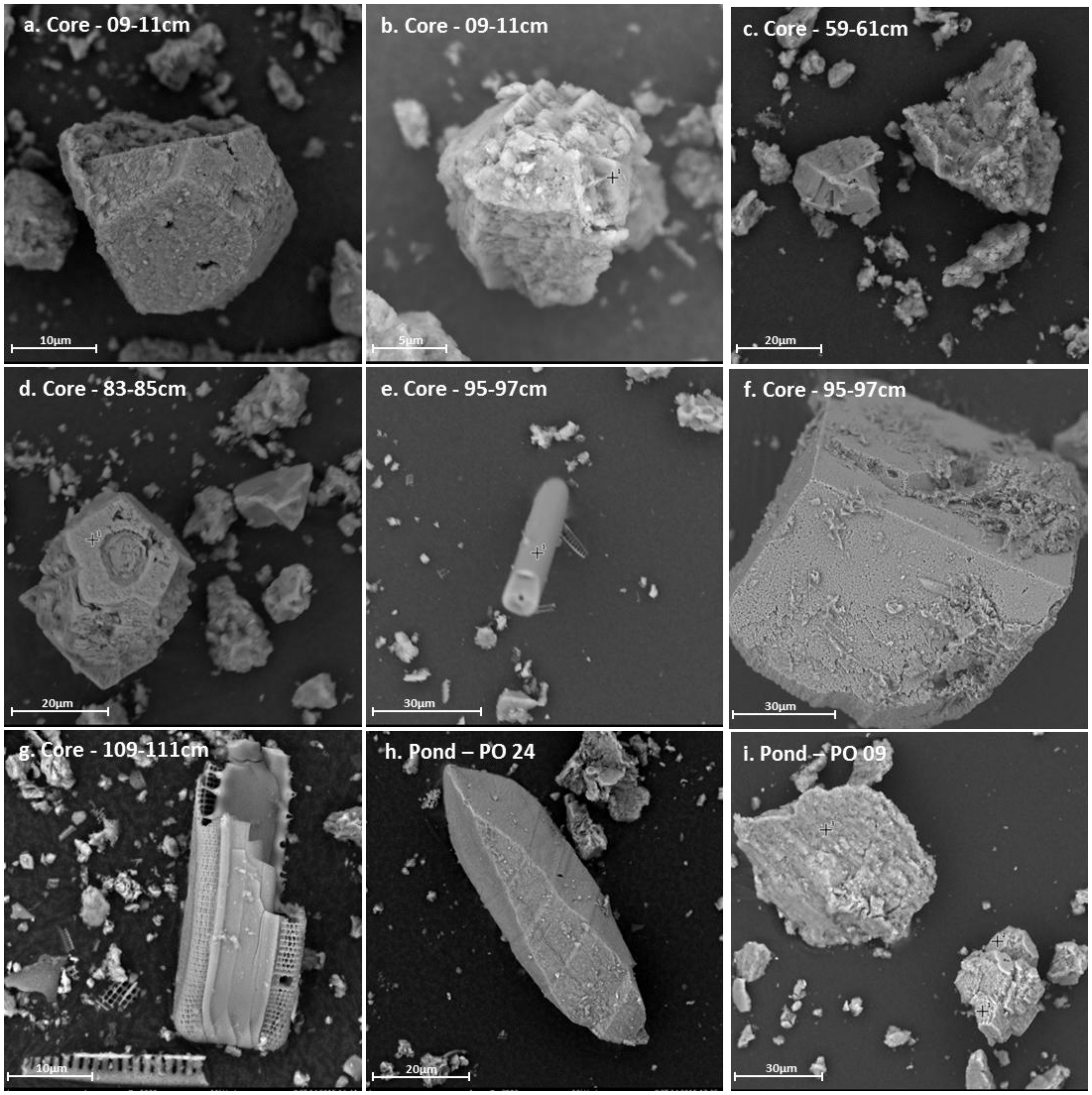

Fig. S4. SEM images of core (a-g) and pond sediment (h-i) in the Louroux pond.

Supplementary data (radionuclides activities, elemental concentrations and $^{87}Sr/^{86}Sr$ ratios)

Table S2. ^{137}Cs activities (Bq kg^{-1}) and thorium concentrations (mg kg^{-1}) in channel bank (CB) and soil (SO) samples.

Sample	^{137}Cs	2σ	Th	2σ
CB 01	2.1	0.1	10.9	0.1
CB 02	2.5	0.2	10.5	0.1
CB 03	1.0	0.2	11.7	0.1
CB 04	0.5	0.1	12.8	0.1
CB 05	0.0	0.3	11.4	0.1
CB 06	1.5	0.1	2.5	0.1
CB 07	0.2	0.1	9.1	0.1
CB 08	1.4	0.2	10.8	0.1
CB 09	0.0	0.3	11.6	0.1
CB 10	0.4	0.1	11.9	0.1
CB 11	0.6	0.1	10.3	0.1
CB 12	2.8	0.2	10.9	0.1
CB 13	3.0	0.2	12.6	0.1
CB 14	2.7	0.2	11.6	0.1
CB 15	2.2	0.2	11.8	0.1
CB 16	1.0	0.2	7.5	0.1
CB 17	1.1	0.2	9.9	0.1
SO 01	3.1	0.2	9.9	0.1
SO 02	3.3	0.2	8.6	0.1
SO 03	5.7	0.2	12.9	0.1
SO 04	2.4	0.1	7.3	0.1
SO 05	2.7	0.1	10.8	0.1
SO 06	1.4	0.1	12.7	0.1
SO 07	2.7	0.1	10.0	0.1
SO 08	2.3	0.2	9.5	0.1
SO 09	6.1	0.1	12.4	0.1
SO 10	2.4	0.1	8.9	0.1
SO 11	2.0	0.2	13.5	0.1
SO 12	5.2	0.2	9.6	0.1
SO 13	4.7	0.2	11.5	0.1
SO 14	2.5	0.2	8.6	0.1
SO 15	3.3	0.2	11.9	0.1
SO 16	3.7	0.2	8.7	0.1
SO 17	2.9	0.2	9.4	0.1
SO 18	3.9	0.2	9.0	0.1
SO 19	8.0	0.3	12.6	0.1
SO 20	1.3	0.2	9.7	0.1
SO 21	3.5	0.2	9.3	0.1
SO 22	3.0	0.2	11.4	0.1
SO 23	3.0	0.2	10.5	0.1
SO 24	1.0	0.1	11.4	0.1
SO 25	2.7	0.2	10.6	0.1
SO 26	3.0	0.2	10.9	0.1

SO 27	3.7	0.2	10.0	0.1
SO 28	3.6	0.2	12.9	0.1
SO 29	2.3	0.2	10.4	0.1
SO 30	2.8	0.2	10.8	0.1
SO 31	4.7	0.3	10.5	0.1
SO 32	3.2	0.3	9.9	0.2
SO 33	4.1	0.4	10.0	0.1
SO 34	3.8	0.3	8.4	0.1
SO 35	2.7	0.3	7.8	0.1
SO 36	2.9	0.3	8.9	0.1

1015 **Table S3. ^{137}Cs activities (Bq kg^{-1}), metal concentrations (mg kg^{-1}) and ^{87}Sr/^{86}Sr ratios in pond sediment samples.**

Sample	^{137}Cs	± 2σ	Th	2σ	Sr	Rb	Ca	Mg	K	Na	Zn	^{87}Sr/^{86}Sr	± 2σ
PO 01	14.1	0.20	15.3	0.1	130	134	37040	5249	12396	1513	102	0.715162	0.000013
PO 07	10.7	0.30	14.4	0.1	103	144	14695	4636	11500	1358	95	0.715162	0.000013
PO 09	2.1	0.30	12.3	0.2	78	119	9099	3985	10712	1526	83	0.716761	0.000018
PO 10	11.1	0.20	11.3	0.1	136	134	28724	4470	11718	1544	99	0.713867	0.000013
PO 12	7.5	0.3	15.8	0.1	129	151	22606	5371	13949	1668	112	0.714598	0.000013
PO 13	6.4	0.20	7.9	0.1	56	65	5361	2744	5848	793	67	0.714839	0.000010
PO 14	4.7	0.20	11.8	0.1	104	125	16297	4393	11241	1578	97	0.715187	0.000010
PO 16	14.9	0.30	10.9	0.1	n.d	n.d	n.d	n.d	n.d	n.d	n.d	n.d	n.d
PO 17	19.9	0.20	14.4	0.1	205	124	62036	4892	11458	1366	106	0.711999	0.000013
PO 18	11.9	0.30	13.9	0.1	123	127	26900	4563	11066	1580	98	0.713984	0.000013
PO 19	5.3	0.3	11.1	0.1	145	134	34003	4545	11676	1634	102	0.713467	0.000013
PO 20	14.4	0.30	12	0.1	161	143	45078	5315	12452	1388	117	0.713192	0.000013
PO 21	13.9	0.40	12	0.1	154	139	40215	5711	13335	1491	120	0.713271	0.000013
PO 22	14.8	0.30	11.1	0.1	151	121	45650	4585	10759	1241	103	0.712866	0.000050
PO 24	6.9	0.30	11.1	0.1	242	95	88855	3851	10418	2379	89	0.711595	0.000021
PO 25	11.6	0.40	10.3	0.1	225	103	76936	4044	10586	2075	93	0.711703	0.000012
PO 26	7.8	0.30	10.7	0.1	224	118	81468	5098	11962	1795	103	0.711656	0.000013
PO 27	16.9	0.30	11.1	0.1	178	132	60768	4943	11341	1439	111	0.712502	0.000013
PO 28	13.1	0.40	11.6	0.1	194	139	65685	5587	12925	1458	118	0.712316	0.000035
PO 29	11.0	0.40	10.8	0.1	207	125	87738	4998	10953	1263	108	0.711904	0.000021
PO 33	19.1	0.4	16.0	0.1	167	144	50201	5466	12582	1304	124	0.713002	0.000021
PO 34	18.9	0.30	15.5	0.1	171	144	52453	5829	13248	1362	116	0.712802	0.000035
PO 36	14.8	0.20	12	0.1	171	147	49430	5827	13375	1312	115	n.d	n.d
PO 38	20.9	0.40	15.6	0.1	170	146	50897	5407	12421	1223	120	0.712973	0.000013
PO 41	16.4	0.3	11.6	0.1	169	145	51324	5744	13328	1363	117	0.712980	0.000021
PO 42	1.2	0.10	2.8	0.1	44	21	11515	731	2605	366	22	0.712325	0.000013
PO 43	14.1	0.40	11.7	0.1	167	126	51695	4759	11052	1187	114	0.712534	0.000014
PO 44	11.5	0.20	10.6	0.1	171	138	54392	5212	12007	1195	119	n.d	n.d
PO 46	18.6	0.20	15.3	0.1	166	142	51519	5808	13174	1334	117	n.d	n.d
PO 47	2.3	0.20	12.2	0.1	126	147	24933	5474	13543	1482	111	0.714391	0.000021
PO 48	13.8	0.40	11.6	0.1	n.d	n.d	n.d	n.d	n.d	n.d	n.d	n.d	n.d
PO 49	22.1	0.50	11.7	0.1	113	128	20402	4486	11567	1548	111	0.714711	0.000021
PO 50	23.1	0.50	11.5	0.1	n.d	n.d	n.d	n.d	n.d	n.d	n.d	n.d	n.d
PO 52	13.5	0.4	12.0	0.1	172	140	52189	5757	12957	1311	117	0.712678	0.000035
PO 56	15.9	0.40	15	0.1	n.d	n.d	n.d	n.d	n.d	n.d	n.d	n.d	n.d
PO 57	12.1	0.30	14.8	0.1	251	165	63363	7067	15853	1732	108	0.712151	0.000020
PO 61	8.0	0.20	13.1	0.1	123	77	34491	3290	7966	1099	71	0.712466	0.000021
PO 62	12.6	0.20	15.4	0.1	n.d	n.d	n.d	n.d	n.d	n.d	n.d	n.d	n.d
PO 67	3.6	0.20	7.5	0.1	105	64	48754	3090	6729	845	59	n.d	n.d
PO 70	13.9	0.30	15.6	0.1	168	131	53626	5492	12446	1288	115	0.712584	0.000021
PO 71	17.0	0.30	15.3	0.1	n.d	n.d	n.d	n.d	n.d	n.d	n.d	n.d	n.d
PO 73	16.8	0.30	14.8	0.1	175	133	57136	5513	12565	1328	113	0.712509	0.000021

1016

1017 **Table S4. ^{137}Cs activities (Bq kg^{-1}), metal concentrations (mg kg^{-1}) and ^{87}Sr/^{86}Sr ratios in core sediment samples.**

Sample	^{137}Cs	2σ	Th	2σ	Sr	Rb	Ca	Mg	K	Na	Zn	^{87}Sr/^{86}Sr	± 2σ
CO 2-3cm	11.3	0.6	12.1	0.2	184	140	61263	5390	11806	1477	96	0.712444	0.000022
CO 5-6cm	10.9	0.7	12.0	0.3	n.d	n.d	n.d	n.d	n.d	n.d	n.d	n.d	n.d
CO 9-10cm	11.9	0.7	13.1	0.3	187	142	60711	5339	11797	1492	100	0.712364	0.000022
CO 12-13cm	14.8	0.6	12.9	0.2	n.d	n.d	n.d	n.d	n.d	n.d	n.d	n.d	n.d
CO 15-16cm	16.3	0.6	12.7	0.2	168	154	52624	5606	12324	1498	102	0.712900	0.000015
CO 18-19cm	18.0	0.7	12.5	0.2	n.d	n.d	n.d	n.d	n.d	n.d	n.d	n.d	n.d
CO 21-23cm	18.0	0.7	13.2	0.2	180	151	60354	5456	12225	1540	102	0.712624	0.000015
CO 23-24cm	21.2	0.7	12.5	0.2	180	153	59930	5419	12116	1503	101	0.712723	0.000011
CO 26-27cm	24.8	0.7	11.7	0.2	173	149	57242	5446	12133	1527	95	0.712771	0.000011
CO 28-29cm	33.7	0.8	11.0	0.2	n.d	n.d	n.d	n.d	n.d	n.d	n.d	n.d	n.d
CO 29-31cm	44.2	0.9	11.9	0.2	190	146	67605	5216	11385	1463	96	0.712318	0.000010
CO 31-33cm	9.7	0.5	13.0	0.2	140	158	49675	5443	12746	1931	86	0.714132	0.000010
CO 33-34cm	**0.0**	0.8	14.4	0.2	n.d	n.d	n.d	n.d	n.d	n.d	n.d	n.d	n.d
CO 35-37cm	**0.0**	0.6	14.2	0.2	109	149	36897	5515	12660	2120	73	0.716028	0.000009
CO 39-41cm	**0.0**	0.8	14.1	0.2	n.d	n.d	n.d	n.d	n.d	n.d	n.d	n.d	n.d
CO 41-43cm	0.9	0.3	14.9	0.	98	143	27734	5473	12594	2210	72	0.716864	0.000012
CO 45-47cm	**0.0**	0.5	14.1	0.2	n.d	n.d	n.d	n.d	n.d	n.d	n.d	n.d	n.d
CO 47-49cm	**0.0**	0.6	13.9	0.2	98	141	32275	5002	12824	2665	70	0.716415	0.000013
CO 50-52cm	1.6	0.3	12.4	0.1	n.d	n.d	n.d	n.d	n.d	n.d	n.d	n.d	n.d
CO 53-55cm	8.1	0.5	12.4	0.2	117	120	40927	4698	10633	1886	64	0.714503	0.000009
CO 56-58cm	14.4	0.7	12.5	0.2	n.d	n.d	n.d	n.d	n.d	n.d	n.d	n.d	n.d
CO 59-61cm	7.2	0.5	13.5	0.2	132	132	51015	4973	11544	1896	65	0.714249	0.000014
CO 62-64cm	7.0	0.4	12.1	0.2	n.d	n.d	n.d	n.d	n.d	n.d	n.d	n.d	n.d
CO 65-67cm	4.8	0.4	13.1	0.2	137	126	61095	4938	11741	2120	61	0.714011	0.000012
CO 68-70cm	5.5	0.4	12.0	0.2	n.d	n.d	n.d	n.d	n.d	n.d	n.d	n.d	n.d
CO 71-73cm	7.2	0.3	13.0	0.1	n.d	n.d	n.d	n.d	n.d	n.d	n.d	n.d	n.d
CO 77-79cm	0.0	0.5	13.8	0.2	114	125	52624	4661	11951	2483	65	0.714868	0.000014
CO 83-85cm	0.0	0.7	13.3	0.2	170	129	60557	7049	17460	2852	66	0.713423	0.000013
CO 89-91cm	0.0	0.8	10.9	0.2	163	117	63053	4390	14036	2909	61	0.713076	0.000012
CO 95-97cm	0.0	0.9	11.3	0.3	206	114	105272	5617	14287	2876	56	0.712320	0.000013
CO 101-103cm	0.0	0.6	11.6	0.2	114	105	42044	4815	11168	1879	72	0.714075	0.000013
CO 109-111cm	2.9	0.5	9.6	0.2	322	90	144826	3693	8377	1445	47	0.710739	0.000012

1018

1019

1020

1021

1022

1023

1024

1025 **Table S5. Selective extraction - $^{87}Sr/^{86}Sr$ ratios, calcium and strontium concentrations (mg kg^{-1}) in the F1 fraction of**
1026 **triplicate core sediment samples.**

Sample	$^{87}Sr/^{86}Sr$	± 2σ	Ca	Sr
CO 9-10cm (1)	0.709391	1.47E-05	50404	125
CO 9-10cm (2)	0.709389	1.47E-05	50099	125
CO 9-10cm (3)	0.709395	1.47E-05	53663	131
CO 23-24cm (1)	0.709393	1.47E-05	53878	125
CO 23-24cm (2)	0.709401	1.47E-05	50499	119
CO 23-24cm (3)	0.709347	1.47E-05	51741	123
CO 29-31cm (1)	0.709395	1.41E-05	62834	143
CO 29-31cm (2)	0.709395	1.41E-05	57591	130
CO 29-31cm (3)	0.709393	1.15E-05	62520	140
CO 41-43cm (1)	0.709388	1.47E-05	25859	43
CO 41-43cm (2)	0.709378	1.47E-05	24754	41
CO 41-43cm (3)	0.709368	1.47E-05	25620	43
CO 59-61cm (1)	0.709393	1.47E-05	44063	79
CO 59-61cm (2)	0.709379	1.43E-05	42247	75
CO 59-61cm (3)	0.709359	1.43E-05	43010	78
CO 83-85cm (1)	0.709343	1.43E-05	51102	112
CO 83-85cm (2)	0.709348	1.43E-05	47719	103
CO 83-85cm (3)	0.709334	1.43E-05	47192	103
CO 95-97cm (1)	0.709222	1.41E-05	66972	146
CO 95-97cm (2)	0.709210	1.41E-05	69049	150
CO 95-97cm (3)	0.709216	1.41E-05	70905	156
CO 109-111cm (1)	0.709228	1.20E-05	89614	182
CO 109-111cm (2)	0.709237	1.25E-05	89057	180
CO 109-111cm (3)	0.709244	1.02E-05	88587	180

1027

1028 **Table S6. Metal concentrations (mg kg^{-1}) and $^{87}Sr/^{86}Sr$ ratios in shelly sand. carbonate rocks and fertilizers samples.**

Sample	Th	Sr	Rb	Ca	Mg	K	Na	Zn	$^{87}Sr/^{86}Sr$	± 2σ
Shelly sand	n.d	344	20.0	65358	669	3784	646	3.6	0.709538	0.00001
CA 01	n.d	195	0.7	411776	4903	886	143	4.7	0.708706	0.00002
CA 02	n.d	176	0.5	380580	4411	1854	185	4.0	0.708716	0.00002
CA 03	n.d	195	n.d	403733	n.d	n.d	120	n.d	0.708789	0.00001
CA 04	n.d	404	1.3	380590	5168	1064	718	1.4	0.708708	0.00001
CA 05	n.d	485	1.1	528816	6378	1113	291	1.9	0.708698	0.00002
CA 06	n.d	353	n.d	379283	n.d	n.d	121	n.d	0.708743	0.00003

1029

Sample	Th	Sr	Rb	Ca	Mg	K	Na	Zn	$^{87}Sr/^{86}Sr$	± 2σ
Fertilizer - N (33.5)	0.3	0.4	0.9	<	<	<	2388	1.1	0.716224	0.000241
Fertilizer - N.P.K (15.15.15)	0.5	65	27	16887	4631	110575	3358	136	0.707877	0.002812
Fertilizer - P.K (25.25)	5.6	504	19	92102	5650	138238	13912	184	0.709178	0.000014

1030

1031